

DOI:10.1002/ejic.201201403

# Synthesis, Characterization, and Dynamic Behaviour of Triosmium Clusters Containing the Tridentate Ligand $\{\text{Ph}_2\text{PCH}_2\text{CH}_2\}_2\text{S}$ (PSP)

Roger Persson,<sup>[a]</sup> Marc J. Stchedroff,<sup>[a,b]</sup> Roberto Gobetto,<sup>[b]</sup> Carl J. Carrano,<sup>[c]</sup> Michael G. Richmond,<sup>[d]</sup> Magda Monari,<sup>[e]</sup> and Ebbe Nordlander\*<sup>[a]</sup>

**Keywords:** Cluster compounds / Osmium / Tridentate ligands / P,S ligands / Isomerization

Reaction of  $[\text{Os}_3(\text{CO})_{11}(\text{NCMe})]$  with bis-diphenylphosphanylene ethylene sulfide,  $\{\text{Ph}_2\text{PCH}_2\text{CH}_2\}_2\text{S}$  (PSP), leads to the formation of  $[\text{Os}_3(\text{CO})_{11}(\text{PSP})]$  and  $[\{\text{Os}_3(\text{CO})_{11}\}_2(\mu\text{-PSP})]$  in good yield. Similarly, treatment of  $[\text{Os}_3(\text{CO})_{10}(\text{NCMe})_2]$  with PSP affords the cluster  $[\text{Os}_3(\text{CO})_{10}(\mu\text{-PSP})]$ , in which the two phosphanes of the PSP ligand coordinate to different osmium atoms of the same triosmium unit. Reaction of  $[\text{Os}_3(\text{CO})_{11}(\text{PSP})]$  with  $[\text{Os}_3(\text{CO})_{10}(\text{NCMe})_2]$  yields the compound  $1,2-\{[\text{Os}_3(\text{CO})_{11}](\mu_3\text{-PSP})\{[\text{Os}_3(\text{CO})_{10}]\}$  in which the thioether moiety and one of the phosphane groups of the PSP ligand are coordinated equatorially to the  $\{[\text{Os}_3(\text{CO})_{10}]\}$  subunit. The cluster  $1,2-\{[\text{Os}_3(\text{CO})_{11}](\mu_3\text{-PSP})\{[\text{Os}_3(\text{CO})_{10}]\}$  is also formed

when  $[\text{Os}_3(\text{CO})_{11}(\text{PSP})]$  is oxidatively decarbonylated by reaction with trimethylamine *N*-oxide. The metastable cluster  $1,2-\{[\text{Os}_3(\text{CO})_{11}](\mu_3\text{-PSP})\{[\text{Os}_3(\text{CO})_{10}]\}$  undergoes slow isomerisation at room temperature to form  $1,1-\{[\text{Os}_3(\text{CO})_{11}](\mu_3\text{-PSP})\{[\text{Os}_3(\text{CO})_{10}]\}$  in which the thioether and phosphane moieties coordinate in a chelating mode to one of the  $\{[\text{Os}_3(\text{CO})_{10}]\}$  subunits with the thioether moiety in an axial position. The dynamic behaviour of these clusters has been investigated by variable-temperature  $^{13}\text{C}\{^1\text{H}\}$  and  $^{13}\text{P}\{^1\text{H}\}$  NMR spectroscopy. The solid-state structures of  $[\{\text{Os}_3(\text{CO})_{11}\}_2(\mu\text{-PSP})]$  and  $[\text{Os}_3(\text{CO})_{10}(\mu\text{-PSP})]$  are reported.

## Introduction

The coordination of multidentate phosphanes to metal clusters has been thoroughly studied.<sup>[1–4]</sup> Smith,<sup>[3c,5,6]</sup> Lewis,<sup>[2,7]</sup> Deeming,<sup>[8]</sup> Kabir<sup>[9]</sup> and their co-workers have investigated a number of diphosphane-substituted derivatives of  $[\text{Os}_3(\text{CO})_{12}]$  that involve the ligands  $\text{Ph}_2\text{P}(\text{CH}_2)_n\text{PPh}_2$  ( $n = 1–5$ ). Many studies have been carried out on the correlation between the chain length of such phosphane ligands and their coordination modes as well as the dynamics of the clusters. Correlations between the chemical shifts of the phosphorus nuclei and the chain lengths of polydentate

phosphane ligands in both poly- and mononuclear complexes have also been detected.<sup>[10]</sup> However, less attention has been paid to mixed-donor ligands. Multidentate phosphane–thiol or phosphane–thioether (P,S) ligands have been the focus of considerable interest because they are inherently asymmetric and potentially hemilabile. Such ligands have been shown to be potentially useful in catalytic alkylation, carbonylation and coupling reactions.<sup>[11,12]</sup> Investigations into the interactions of P,S ligands with transition-metal carbonyl clusters remain scarce, with the notable exception of the cluster chemistry of thienylphosphanes.<sup>[13,14]</sup>

We have studied the coordination chemistry of some phosphane–thioether ligands with osmium clusters.<sup>[15]</sup> In our study of the ligand  $\text{Ph}_2\text{PCH}_2\text{CH}_2\text{SMe}$  (PS) with regard to triosmium clusters, we found that (i) the thioether moiety of the P,S ligand can only coordinate to a metal centre when the phosphane is already coordinated and (ii) the (kinetically favoured) cluster  $1,2-\{[\text{Os}_3(\text{CO})_{10}](\mu\text{-PS})\}$  slowly converts to the thermodynamically favoured cluster  $1,1-\{[\text{Os}_3(\text{CO})_{10}](\text{PS})\}$  in solution.<sup>[15a]</sup> Although many mononuclear metal complexes that contain the ligand bis-diphenylphosphanylene ethylene sulfide  $\{\text{Ph}_2\text{PCH}_2\text{CH}_2\}_2\text{S}$  (PSP) have been prepared,<sup>[16]</sup> there are, to the best of our knowledge, no reports of coordination of PSP to transition-metal clusters. We were interested in investigating the coordination

[a] Inorganic Chemistry Research Group, Chemical Physics, Center for Chemistry and Chemical Engineering, Lund University, Box 124, 22100 Lund, Sweden  
Fax: +46-46-222-4119  
E-mail: Ebbe.Nordlander@chemphys.lu.se  
Homepage: <http://www.chemphys.lu.se/people/nordlander>

[b] Dipartimento di Chimica, Università di Torino, Via P. Giuria 7, 10125 Torino, Italy

[c] Department of Chemistry and Biochemistry, San Diego State University, 5500 Campanile Drive, San Diego, CA 92182-1030, USA

[d] Department of Chemistry, University of North Texas, 1155 Union Circle, Box 305070, Denton, TX 76203, USA

[e] Dipartimento di Chimica “G. Ciamician”, Università degli Studi di Bologna, Via Selmi 2, 40126 Bologna, Italy

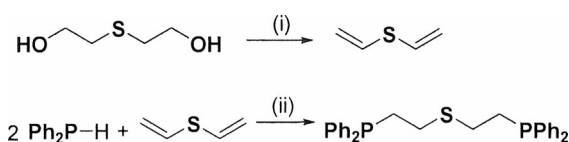
Supporting information for this article is available on the WWW under <http://dx.doi.org/10.1002/ejic.201201403>.

chemistry of PSP with polynuclear transition-metal complexes; in particular, we wanted to ascertain to what extent the thioether moiety might compete with the phosphanes as a ligand to one or several transition metal(s) in a low-oxidation state. Herein, we wish to describe the products of the reaction of PSP with the mono- and bis-acetonitrile derivatives of  $[\text{Os}_3(\text{CO})_{12}]$ <sup>[17,18]</sup> as well as further reactions of the resultant products.

## Results and Discussion

### Preparation of $\{\text{Ph}_2\text{PCH}_2\text{CH}_2\}_2\text{S}$ (PSP)

The original method of preparation of PSP involves phosphination of bis(2-chloroethylene)sulfide by the diphenylphosphide anion.<sup>[16d]</sup> The disadvantage of this method is the toxicity of bis(2-chloroethylene)sulfide (sulfur mustard). We therefore developed an alternative route to PSP that is based on the general method of anti-Markovnikov addition of a P–H (or an S–H or N–H) bond to a carbon–carbon double bond, which has been used for the preparation of a wide range of polydentate tertiary phosphanes as well as P,S- and P,N-type bidentate ligands.<sup>[19]</sup> Thus, PSP was prepared by free-radical-catalysed addition of diphenylphosphane to divinyl sulfide as shown in Scheme 1. The conversion of divinyl sulfide to PSP was almost quantitative according to  $\{^1\text{H}\}^{31}\text{P}$  and  $^1\text{H}$  NMR spectroscopy of the crude product. The product was slightly contaminated by the corresponding phosphane oxide(s), which could be removed by chromatography, and the isolated yield was only moderate (49%) owing to some decomposition on and incomplete extraction from the column. Attempts to prepare PSP by means of the condensation of  $\text{PPh}_2\text{CH}_2\text{CH}_2\text{SH}$  with  $\text{PPh}_2\text{CH}=\text{CH}_2$  did not give good results.



Scheme 1. Preparation of PSP: (i) KOH, 150–200 °C; (ii) AIBN, 120 °C, 1 h.

### Synthesis and Characterisation of $[\text{Os}_3(\text{CO})_{11}(\text{PSP})]$ (**1**) and $\{[\text{Os}_3(\text{CO})_{11}]_2(\mu\text{-PSP})\}$ (**2**)

Reaction of  $[\text{Os}_3(\text{CO})_{11}(\text{NCMe})]$  with PSP in  $\text{CH}_2\text{Cl}_2$  at room temperature affords a mixture of two compounds, namely, orange **1** and yellow **2**. The yields of the respective compounds are dependent on the molar ratio between the reactants; this suggests that the reactions of  $[\text{Os}_3(\text{CO})_{11}(\text{NCMe})]$  with PSP (to form **1**) and with **1** (to form **2**) are competing reactions. Thus, by using two equivalents or more of  $[\text{Os}_3(\text{CO})_{11}(\text{NCMe})]$ , compound **2** is formed in high yield although a small amount of **1** is present as a side product even when an excess amount of  $[\text{Os}_3(\text{CO})_{11}$

(NCMe)] is used. Conversely, the formation of **2** cannot be eliminated by using an excess amount of the PSP ligand. The same observations have been made for the reaction between  $[\text{Os}_3(\text{CO})_{11}(\text{NCMe})]$  and  $\text{Ph}_2\text{P}(\text{CH}_2)_5\text{PPh}_2$  (dppp), which is isostructural to the PSP ligand.<sup>[9]</sup>

The solution IR spectra of **1** and **2** show very similar carbonyl stretching patterns, thus indicating that they possess equivalent symmetry with respect to the carbonyl ligands. The IR spectra also correspond well to those of  $[\text{Os}_3(\text{CO})_{11}(\text{dppp})]$  and  $\{[\text{Os}_3(\text{CO})_{11}]_2(\mu\text{-dppp})\}$  and are thus consistent with the PSP ligand being coordinated through its phosphane moieties in equatorial positions in both clusters.<sup>[5,8,20]</sup> The observation of four resonances for the methylene protons in the  $^1\text{H}$  NMR spectrum of **1** (see the Exp. Sect.) is consistent with the PSP ligand being coordinated in a monodentate “dangling” mode. Similarly, the presence of only two resonances in the methylene region of the  $^1\text{H}$  NMR spectrum of **2** indicates that the PSP ligand is bridging two  $\{\text{Os}_3(\text{CO})_{11}\}$  cluster units. Two singlets at  $\delta = -10.89$  and  $-16.63$  ppm are observed in the  $^{31}\text{P}\{^1\text{H}\}$  NMR spectrum of **1**. The lower frequency (high-field) singlet is assigned to the uncoordinated phosphorus of PSP (compared with free PSP:<sup>[16b]</sup>  $\delta = -16.7$  ppm), whereas that at higher frequency (lower field) is attributed to the coordinated phosphorus atom. This assignment has been confirmed by the determination of  $^1J$  and  $^2J$   $^{31}\text{P}$ ,<sup>187}\text{Os} coupling constants for **1** (223 and 53 Hz, respectively, at 303 K).<sup>[21]</sup></sup>

Only one singlet at  $\delta = -10.7$  ppm is present in the  $^{31}\text{P}\{^1\text{H}\}$  NMR spectrum of **2**, thus indicating one single phosphorus environment. The shift agrees with the low-field resonance of **1**, which suggests that both phosphorus atoms are coordinated in **2**. The fast-atom bombardment (FAB) mass spectra of **1** and **2** agree with the formulations  $[\text{Os}_3(\text{CO})_{11}(\text{PSP})]$  and  $\{[\text{Os}_3(\text{CO})_{11}]_2(\mu\text{-PSP})\}$ , respectively. The above-mentioned spectroscopic data are in complete agreement with the expected structures for **1** and **2**, which are depicted in Figure 1.

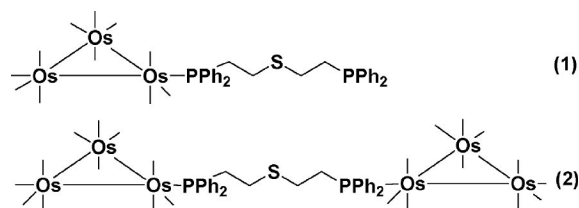


Figure 1. Proposed structures of  $[\text{Os}_3(\text{CO})_{11}(\text{PSP})]$  (**1**) and  $\{[\text{Os}_3(\text{CO})_{11}]_2(\mu\text{-PSP})\}$  (**2**).

### Carbonyl Fluxionality in **1**

The room-temperature (293 K)  $^{13}\text{C}$  NMR spectrum of **1** reveals that the carbonyl ligands are fluxional. To freeze out this fluxionality and determine its mechanism, a variable-temperature study was carried out. The low-temperature (213 K) limiting  $^{13}\text{C}\{^1\text{H}\}$  NMR spectrum of **1** shows eight singlets downfield of  $\delta = 169$  ppm with intensity ratios 2:2:2:1:1:1:1:1 (Figure 2) in the carbonyl region. Six carb-

onyl resonances – two attributed to axial CO signals (relative intensity 2) at  $\delta = 192.4$  ( $^2J_{\text{P,CO}} = 8$  Hz) and 184.7 ppm, and two equatorial CO signals (relative intensity 1) at  $\delta = 176.1$  and 169.5 ppm – undergo a concerted collapse around 253 K (see Figure 2); this is consistent with a classical “merry-go-round” process, as outlined in Figure 3.<sup>[22,23]</sup> On increasing the temperature to 293 K, all the remaining resonances broaden. The Gibbs’ free energies of activation ( $\Delta G^\ddagger$ ) for the merry-go-round process(es) were calculated to be  $50.3(\pm 1)$  kJ mol<sup>-1</sup> for the process that involves carbonyl ligands **a/a'**, **f/f'**, **b** and **g**, and  $59.4(\pm 1)$  kJ mol<sup>-1</sup> for the process that involves carbonyl ligands **c,c'**, **f,f'**, **d** and **h** (see Figure 3).

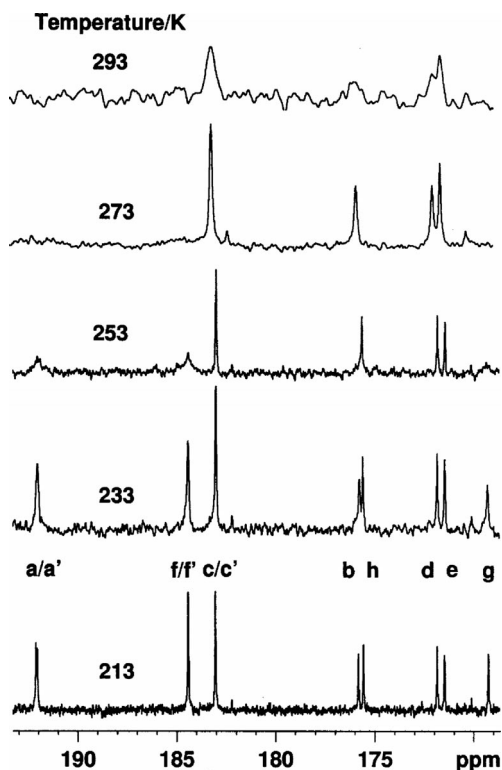


Figure 2. Variable-temperature  $^{13}\text{C}\{^1\text{H}\}$  NMR spectra (126 MHz,  $\text{CDCl}_3$ , 213 K) of **1** showing fluxionality consistent with that described in Scheme 2.

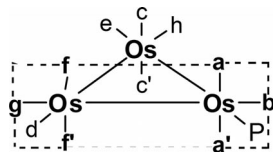


Figure 3. The fluxional CO process of **1**.

For the related cluster  $[\text{Os}_3(\text{CO})_{11}\{\text{P}(\text{OMe})_3\}]$ , Pomeroy and co-workers<sup>[23]</sup> were able to distinguish three distinct dynamic processes with significantly different activation energies. Two of these processes were of the merry-go-round type, which operate at lower temperatures and do not involve the phosphite ligand, whereas the third, a turnstile mechanism that involves phosphite liberation, was found to operate at significantly higher temperatures. The assign-

ment of the resonances in the low-temperature (213 K) limiting  $^{13}\text{C}\{^1\text{H}\}$  spectrum of **1** was accomplished by studying the temperature dependence of the carbonyl resonances of **1** and by comparing the  $^{13}\text{C}\{^1\text{H}\}$  NMR spectrum of **1** with the related clusters  $[\text{Os}_3(\text{CO})_{11}\text{PS}]$ <sup>[14]</sup> and  $[\text{Os}_3(\text{CO})_{11}\text{-P}(\text{OMe})_3]$ .<sup>[23]</sup>

## Crystal and Molecular Structure of **2**

It was possible to grow crystals of **2** suitable for single-crystal X-ray crystallography, and its crystal structure was determined to confirm the proposed structure. The molecular structure is shown in Figure 4 and relevant bond lengths and angles are reported in Table 1. The molecule consists of two  $\{\text{Os}_3(\text{CO})_{11}\}$  units linked by the PSP ligand. The two triosmium triangles are oriented with their faces approximately perpendicular to each other. The phosphorus atoms of the PSP ligand coordinate to equatorial sites of each triosmium unit, as has been previously found in related  $[\text{Os}_3(\text{CO})_{11}(\text{PR}_3)]$  species.<sup>[8b,9,20,24,25]</sup> Bridging dimers of similar structures to **2** have been prepared by treating bidentate phosphanes with triosmium<sup>[9,20]</sup> and triruthenium<sup>[26]</sup> clusters. Dimers that consist of two cluster units linked by other phosphorus-based ligands have also been prepared by treating tri- and tetraphospholanes with activated triosmium clusters.<sup>[27,28]</sup> The sulfur atom and the methylene groups are oriented in a zigzag conformation and the sulfur atom is not within bonding distance to any osmium atom. It has previously been observed that the presence of a bulky  $\text{PR}_3$  group causes a lengthening of the Os–

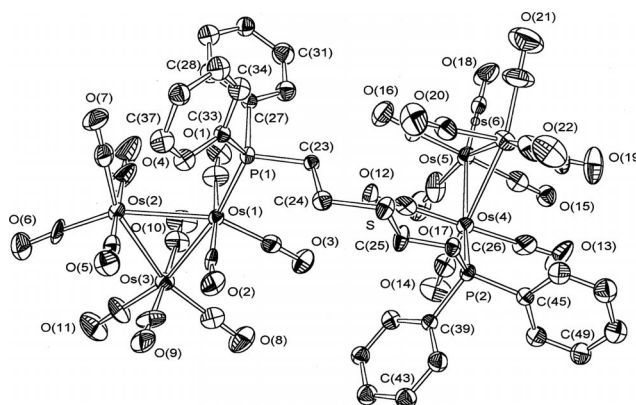


Figure 4. An ORTEP plot of the molecular structure of **2**. Hydrogen atoms have been omitted for clarity. Thermal ellipsoids are at 30% probability level.

Table 1. Selected bond lengths [Å] and angles [°] for **2**.

Os(1)–Os(2)	2.888(1)	Os(4)–P(2)	2.381(2)
Os(1)–Os(3)	2.878(1)	S–C(24)	1.78(1)
Os(2)–Os(3)	2.868(1)	S–C(25)	1.80(1)
Os(4)–Os(5)	2.876(1)	C(23)–C(24)	1.53(1)
Os(5)–Os(6)	2.888(1)	C(25)–C(26)	1.49(1)
Os(4)–Os(6)	2.882(1)	Os–C(ax)	1.91–1.98(1)
Os(1)–P(1)	2.330(2)	Os–C(eq)	1.85–1.95(1)
C(24)–S–C(25)	100.5(3)	C(23)–P(1)–Os(1)	113.7(2)
C(26)–P(2)–Os(4)	118.9(2)		

Os bonds adjacent to the phosphorus atoms<sup>[8,29]</sup> and the two Os–Os bonds *cis* to the phosphorus are indeed slightly longer than the average Os–Os distance in the parent cluster  $[\text{Os}_3(\text{CO})_{12}]$  [2.877(3) Å]<sup>[30]</sup> but only in one triangle is the Os–Os separation *cis* to the P atom the longest one [Os(1)–Os(2) 2.888(1) Å].

As a consequence of the steric hindrance of the PSP ligand, a widening of the angles Os(2)–Os(1)–P(1) and Os(6)–Os(4)–P(2) to 110.21(5) and 106.15(6)°, respectively, is observed. In the parent carbonyl the M–M–CO angles range from 96.1 to 99.9°.<sup>[30]</sup> The Os–P distances [Os(1)–P(1) 2.330(2) Å and Os(2)–P(2) 2.381(2) Å] fall in the range 2.28–2.40 Å, which is typical for these bonds.<sup>[29]</sup> The two equatorial CO ligands bound to the two osmium atoms that are coordinated by the PSP ligand show some shortening of the Os–C distances on account of increased  $\pi$  backbonding from the metal to the CO [Os(1)–C(3) 1.88(1) Å and Os(4)–C(14) 1.85(1) Å].

### Synthesis and Characterisation of $[\text{Os}_3(\text{CO})_{10}(\mu\text{-PSP})]$ (**3**)

Cluster **3** is formed in moderate yield through treatment of  $[\text{Os}_3(\text{CO})_{10}(\text{NCMe})_2]$  with PSP in  $\text{CHCl}_3$  heated at reflux. It is also possible to form **3** by oxidative decarbonylation of **1** by using the oxygen-transfer reagent  $\text{Me}_3\text{NO}$ .<sup>[18]</sup> Both reactions produce several minor products, which remain uncharacterised. Cluster **3** exhibits an  $\nu_{\text{CO}}$  IR pattern similar to that of  $[\text{Os}_3(\text{CO})_{10}\{\mu\text{-Ph}_2\text{P}(\text{CH}_2)_n\text{PPh}_2\}]$  ( $n = 1, 4$ ).<sup>[8,20]</sup> One singlet at  $\delta = -4.26$  ppm was observed in the  $^{31}\text{P}\{\text{H}\}$  NMR spectrum of **3**, a shift to higher frequency by approximately 12 ppm relative to the free PSP ligand. This shift difference is approximately twice as large as that observed for **1** and **2**; the additional shift might be due to a ring contribution effect<sup>[10]</sup> as the phosphorus atom is part of a nine-membered ring (see below). The FAB mass spectrum of **3** is in agreement with the formulation  $[\text{Os}_3(\text{CO})_{10}(\mu\text{-PSP})]$  and the expected structure is depicted in Figure 5.

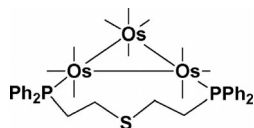


Figure 5. Proposed structure of **3**.

### Crystal and Molecular Structure of **3**

The crystal structure of **3** was determined to confirm its proposed structure and compare it to related  $[\text{Os}_3(\text{CO})_{10}(\mu\text{-diphosphane})]$  clusters. The molecular structure is shown in Figure 6 and selected bond lengths and angles for **3** are listed in Table 2. Cluster **3** consists of a triangular triosmium cluster with ten terminal carbonyl ligands and the PSP ligand bridging one Os–Os edge.

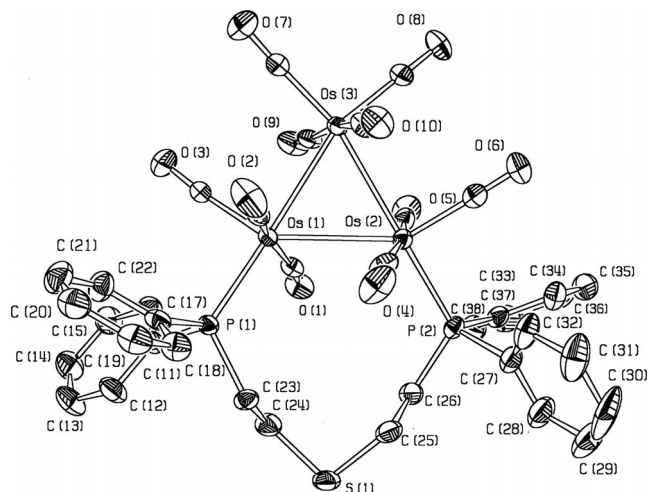


Figure 6. An ORTEP plot of the molecular structure of **3**. Hydrogen atoms have been omitted for clarity. Thermal ellipsoids are at the 30% probability level.

Table 2. Selected bond lengths [Å] and angles [°] for **3**.

Os(1)–Os(2)	2.9687(3)	Os(1)–C(3)	1.884(6)
Os(1)–Os(3)	2.8707(3)	Os(2)–C(4)	1.935(6)
Os(2)–Os(3)	2.8834(3)	Os(2)–C(5)	1.967(6)
Os(1)–P(1)	2.343(1)	Os(2)–C(6)	1.876(7)
Os(2)–P(2)	2.348(1)	Os(3)–C(7)	1.888(7)
S(1)–C(24)	1.804(6)	Os(3)–C(8)	1.906(6)
S(1)–C(25)	1.816(6)	Os(3)–C(9)	1.951(6)
Os(1)–C(1)	1.936(6)	Os(3)–C(10)	1.940(6)
Os(1)–C(2)	1.950(6)	C–O <sub>ax</sub> (range)	1.114–1.148(7)
C–O <sub>eq</sub> (range)	1.134–1.155(7)		
Os(2)–Os(1)–P(1)	122.56(3)	Os(1)–P(1)–C(23)	119.6(2)
Os(1)–Os(2)–P(2)	121.90(4)	Os(2)–P(2)–C(26)	119.4(2)
C(24)–S(1)–C(25)	98.9(3)		

The molecule conforms to an idealised  $C_2$  symmetry if the phenyl groups attached to the phosphorus atoms are ignored. The two phosphane moieties occupy equatorial sites on different osmium atoms with the phosphorus atoms *cis* to each other. The bridged metal–metal bond [Os(1)–Os(2) 2.969(1) Å] is slightly longer than the two nonbridged ones [Os(2)–Os(3) 2.883(1) Å, Os(1)–Os(3) 2.871(1) Å] as well as the average Os–Os distance in  $[\text{Os}_3(\text{CO})_{12}]$  (Os–Os<sub>av</sub> 2.877 Å).<sup>[30]</sup> Elongation of the bridged Os–Os bond has also been observed in the related compounds  $[\text{Os}_3(\text{CO})_{10}\{\mu\text{-Ph}_2\text{P}(\text{CH}_2)_n\text{PPh}_2\}]$  ( $n = 2, 3, 4, 5$ ),<sup>[31a, b]</sup> in which the diphosphane ligands are bridging one metal–metal bond [bridged Os–Os bonds: 2.891(1), 2.939(1) and 2.965(2) Å for  $n = 2, 4$  and 5, respectively]. The increase in bond length has been ascribed to conformational requirements of the methylene groups of the diphosphane ligand spanning the osmium–osmium bond.<sup>[8]</sup> In the molecular structure of  $[\text{Os}_3(\text{CO})_{10}(\mu\text{-Ph}_2\text{PCH}_2\text{PPh}_2)]$ ,<sup>[31c]</sup> the diphosphane-bridged and unbridged Os–Os bonds are not significantly different [Os–Os<sub>bridged(av)</sub> 2.867 Å and Os–Os<sub>unbridged(av)</sub> 2.870 Å]. The phosphorus–osmium distances in **3** [Os(1)–P(1) 2.332(1), Os(2)–P(2) 2.348(1) Å] are comparable to those in  $[\text{Os}_3(\text{CO})_{10}\{\mu\text{-Ph}_2\text{P}(\text{CH}_2)_n\text{PPh}_2\}]$  ( $n = 1, 2, 4, 5$ ): Os–P<sub>av</sub>: 2.324, 2.330,

2.348 and 2.338 Å for  $n = 1, 2, 4, 5$ , respectively.<sup>[31]</sup> As found in cluster **2**, the sulfur atom is not within bonding distance to any osmium atom.

The two methylene groups next to each phosphorus atom are placed on different sides of the triosmium plane because of the presence of the idealised  $C_2$  axis. The carbon–osmium bonds for axial carbonyls [ $Os-C_{av} \approx 1.95$  Å] are slightly longer than the carbon–osmium distances for equatorial carbonyls [ $Os-C_{av} \approx 1.89$  Å]. A further point of interest in the structure of **3** is the twist of the cluster ligand sphere; the four ligands at each metal atom maintain approximately octahedral geometry, but are twisted as a whole with respect to each other. This type of distortion is commonly observed for derivatives of  $[M_3(CO)_{12}]$  ( $M = Ru, Os$ ) and is attributed to steric interactions between the ligands that occur upon introduction of relatively bulky ligands<sup>[32–34]</sup> (e.g., phosphanes/phosphites).<sup>[29]</sup> Such distortion of the metal–carbonyl framework has also been observed for the related compounds  $[Os_3(CO)_{10}\{\mu-Ph_2P(CH_2)_n PPh_2\}]$  ( $n = 1, 2, 4, 5$ ).<sup>[8,20,31]</sup> When toluene was used as a solvent, **3** crystallised as a racemate of a conformer with crystallographically imposed  $C_2$  symmetry (monoclinic, space group  $C2/c$ ; see the Supporting Information).

### Synthesis and Characterisation of 1,1- $\{[Os_3(CO)_{11}]\{\mu-PSP\}\{Os_3(CO)_{10}\}$ (**4a**)

Cluster **4a** is afforded in good yield when  $[Os_3(CO)_{10}(NCMe)_2]$  is treated with **1** in  $CH_2Cl_2$  at room temperature. Compound **4a** was also synthesised by adding a solution of  $Me_3NO$  in  $CH_2Cl_2$  to a solution of **2** in  $CH_2Cl_2$  at room temperature. Multiplets in the area between  $\delta = 2.5$  and 3.1 ppm in the  $^1H$  NMR spectrum of **4a** are attributed to the methylene protons of the asymmetrically bridging PSP ligand. Two singlets at equal intensities were detected at  $\delta = 39.25$  and  $-11.76$  ppm in the  $^{31}P\{^1H\}$  NMR spectrum of **4a**. The high-field signal is comparable to those observed for **1** and **2**, which suggests that a part of the compound consists of one triosmium triangle with an equatorially coordinated phosphane group. The unusual shift for the resonance found at  $\delta = 39.25$  ppm is similar to that of the singlet observed for 1,1- $[Os_3(CO)_{10}(\mu-PPh_2CH_2CH_2SMe)]$  at  $\delta = 38.1$  ppm<sup>[15a]</sup> (see below) and indicates that there might be a ring-contribution effect<sup>[10]</sup> to the shift of the second phosphorus atom. This is consistent with the hypothesis that **4a** consists of two cluster units bridged by a PSP ligand with one phosphane group coordinating to one trinuclear unit and the thioether and second phosphane moieties coordinating to the second osmium triangle. The FAB mass spectrum of **4a** is consistent with the formulation  $[Os_6(CO)_{21}(PSP)]$ .

Two likely isomers exist for  $[\{Os_3(CO)_{11}\}(\mu-PSP)\{Os_3(CO)_{10}\}]$  (**4a** and **4b**), and these structures differ in the coordination mode of the  $-SCH_2CH_2PPh_2$  part of the PSP ligand to the  $\{Os_3(CO)_{10}\}$  unit of the product. In the 1,1-coordination mode, the  $-SCH_2CH_2PPh_2$  moiety chelates one metal atom so that the phosphane is in an

equatorial position and the thioether moiety is in an axial one (isomer **4a**; Figure 7), whereas in the 1,2-coordination mode, the  $-SCH_2CH_2PPh_2$  moiety spans a metal–metal bond and both the thioether and phosphane moieties are coordinated in equatorial positions (isomer **4b**; Figure 7). It is not possible to make an unambiguous distinction between these two structural isomers on the basis of the above-mentioned spectroscopic data. Both types of isomers have been detected for the related cluster  $[Os_3(CO)_{10}(\mu-PPh_2CH_2CH_2SMe)]$ .<sup>[15a]</sup> For this cluster, it was found that the 1,2-isomer is the less stable (kinetically favoured) form while the 1,1-isomer is the thermodynamically favoured form. The 1,2-isomer is stable in the solid state and could be completely characterised, but it was found that it slowly isomerises to the 1,1-isomer in solution.<sup>[15a]</sup> Comparable ligand reactivity has also been observed when the symmetrical diphosphane ligands 4,5-bis(diphenylphosphanyl)-4-cyclopentene-1,3-dione (bpcd),<sup>[35]</sup> (*Z*)- $Ph_2PCH=CHPPh_2$ ,<sup>[36]</sup> and 2,3-bis(diphenylphosphanyl)-*N-p*-tolylmaleimide (bmi)<sup>[37]</sup> react with the activated cluster  $[Os_3(CO)_{10}(MeCN)_2]$ . Each of the ligands reacts rapidly with  $[Os_3(CO)_{10}(MeCN)_2]$  to form the clusters 1,2- $[Os_3(CO)_{10}(bpcd)]$ , 1,2- $[Os_3(CO)_{10}\{(Z)-Ph_2PCH=CHPPh_2\}]$  and 1,2- $[Os_3(CO)_{10}(bmi)]$  as kinetic products of ligand substitution. In each of these products the diphosphane ligand bridges one metal–metal bond. The bridged clusters undergo isomerisation into the chelated clusters 1,1- $[Os_3(CO)_{10}(bpcd)]$ , 1,1- $[Os_3(CO)_{10}\{(Z)-Ph_2PCH=CHPPh_2\}]$  and 1,1- $[Os_3(CO)_{10}(bmi)]$ . Both phosphane-donor atoms occupy equatorial coordination sites in each of the reported isomeric pair of clusters. On the basis of the kinetic data measured for the reactions, a nondissociative phosphane migration across one of the Os–Os bonds has been proposed.<sup>[35–37]</sup> More recently, the same type of isomerisation reaction that involves the ligand 1,2-bis(diphenylphosphanyl)benzene has been studied, and a concomitant computational study on isomerisation reactions that involve  $[Os_3(CO)_{10}(P-P)]$  [ $P-P =$  diphosphane, e.g., (*Z*)- $Ph_2PCH=CHPPh_2$ ] indicate that the isomerisation occurs by means of a concerted merry-go-round process that involves one of the phosphane moieties and two CO groups.<sup>[38]</sup> Furthermore, similar isomerisation reactions have been detected for diphosphane-substituted clusters of the general formula  $[H_4Ru_4(CO)_{10}(P-P)]$  ( $P-P =$  diphosphane).<sup>[39]</sup>

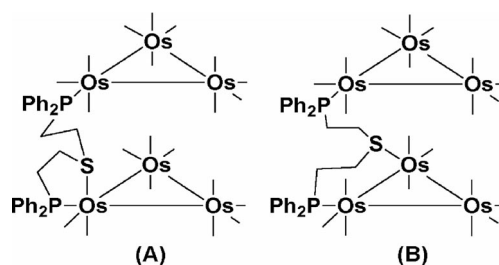


Figure 7. Proposed structures for the two isomers of  $[Os_6(CO)_{21}(PSP)]$ : (A)  $[\{Os_3(CO)_{11}\}\{\mu-(1,1)-PSP\}\{Os_3(CO)_{10}\}]$  (**4a**) and (B)  $[\{Os_3(CO)_{11}\}\{\mu-(1,2)-PSP\}\{Os_3(CO)_{10}\}]$  (**4b**).

Considering the known isomerisation reactions mentioned above, it was thought that both isomeric forms of  $[\{\text{Os}_3(\text{CO})_{11}\}(\mu\text{-PSP})\{\text{Os}_3(\text{CO})_{10}\}]$  might exist and that **4a** might be the (thermodynamically favoured) 1,1-isomer (see Figure 7). To estimate the energy difference between the two isomers, DFT calculations were performed. The geometry-optimised structures for **4a** and **4b** are shown in Figure 8. The calculated free-energy difference between **4a** and **4b** is small ( $1.7 \text{ kcal mol}^{-1}$ ) and favours the 1,1-isomer. The computed  $K_{\text{eq}}$  value at room temperature for the **4a/4b** equilibrium is  $17.7^{-1}$ , which is in excellent agreement with the observation of only cluster **4a** in the NMR spectra of thermally equilibrated samples that contain cluster **4**. The energy difference computed (under identical conditions) for the isomers of  $[\text{Os}_3(\text{CO})_{10}(\mu\text{-PPH}_2\text{CH}_2\text{CH}_2\text{SMe})]$  parallels that found in **4a** and **4b**; here the 1,1-isomer lies  $2.3 \text{ kcal mol}^{-1}$  lower in energy than the 1,2-isomer.<sup>[15c]</sup> The decreased exothermicity in the **4a/4b** isomers relative to the isomeric  $[\text{Os}_3(\text{CO})_{10}(\mu\text{-PPH}_2\text{CH}_2\text{CH}_2\text{SMe})]$  clusters possibly reflects the steric strain associated with the introduction of an extra  $\text{Os}_3(\text{CO})_{11}$  moiety into the former pair of cluster isomers.

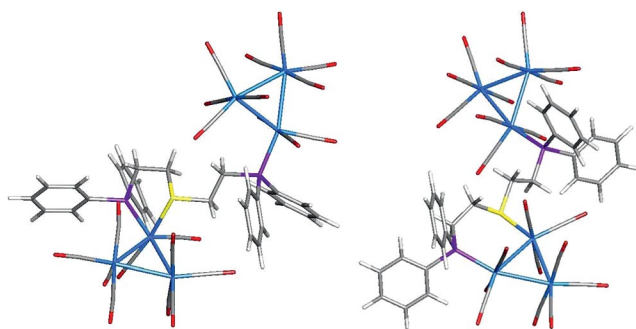


Figure 8. B3LYP-optimised structures for clusters **4a** (left) and **4b** (right).

### Variable-Temperature NMR Spectroscopic Studies of Selectively $^{13}\text{C}$ -Labeled Versions of **4a**

To gain a deeper understanding of the dynamic processes and coordination mode(s) of the PSP ligand in **4a**, a variable-temperature  $^{13}\text{C}\{^1\text{H}\}$  NMR spectroscopic study was undertaken. Because of the large number of possible CO-ligand environments (up to 21), the  $\{\text{Os}_3(\text{CO})_{10}\}$  and  $\{\text{Os}_3(\text{CO})_{11}\}$  cluster subunits of **4a** were selectively enriched by preparing the compounds  $[\{\text{Os}_3(^{13}\text{CO})_{11}\}(\mu\text{-PSP})\{\text{Os}_3(\text{CO})_{10}\}]$  and  $[\{\text{Os}_3(\text{CO})_{11}\}(\mu\text{-PSP})\{\text{Os}_3(^{13}\text{CO})_{10}\}]$  according to the methods employed for the synthesis of **1** and **4a** (see the Exp. Sect.), thus facilitating identification of the resonances due to these subunits and selective observation of the fluxional processes at each subunit. The former compound was made by treating  $[\text{Os}_3(^{13}\text{CO})_{11}(\text{NCMe})]$  with PSP. The enriched version of **1** was isolated from the product and treated further with  $[\text{Os}_3(\text{CO})_{10}(\text{NCMe})_2]$ . The latter compound was obtained from the reaction of **1** with  $[\text{Os}_3(^{13}\text{CO})_{10}(\text{NCMe})_2]$ . The low-temperature  $^{13}\text{C}$  NMR

spectrum of  $1,1-[\{\text{Os}_3(\text{CO})_{11}\}(\mu\text{-PSP})\{\text{Os}_3(^{13}\text{CO})_{10}\}]$  (Figure 9) shows five resonances; one high-frequency (low-field) doublet and four triplets (due to  $^2J_{\text{C,C}}$  couplings) downfield of  $\delta = 185 \text{ ppm}$ , with intensity ratios 1:1:1:1:1 at 185.7 ( $^2J_{\text{C,C}} = 36 \text{ Hz}$ ), 187.4 ( $^2J_{\text{C,C}} = 32 \text{ Hz}$ ), 187.9 ( $^2J_{\text{C,C}} = 36 \text{ Hz}$ ), 190.2 ( $^2J_{\text{C,C}} = 32 \text{ Hz}$ ) and 190.7 ppm ( $^2J_{\text{C,P}} = 6 \text{ Hz}$ ) assigned to axial carbonyls and five resonances upfield of  $\delta = 185 \text{ ppm}$ , with intensity ratios 1:1:1:1:1 at  $\delta = 181.1$ , 178.3, 176.7, 174.2 and 172.9 ppm. The lack of a large  $^2J_{\text{C,C}}$  coupling for the latter resonance indicates that the ligand sulfur (rather than a carbonyl ligand) is axially coordinated in the  $\{\text{Os}_3(\text{CO})_{10}\}$  unit of **4a**. The overall pattern of the  $^{13}\text{C}$  NMR spectrum of  $[\{\text{Os}_3(\text{CO})_{11}\}(\mu\text{-PSP})\{\text{Os}_3(^{13}\text{CO})_{10}\}]$  resembles that of  $1,1-[\text{Os}_3(\text{CO})_{10}(\text{PS})]$  (PS =  $\text{Ph}_2\text{PCH}_2\text{CH}_2\text{SMe}$ ; see above).<sup>[15a]</sup> The only difference is the appearance of the doublet at  $\delta = 190.7 \text{ ppm}$  for  $[\{\text{Os}_3(\text{CO})_{11}\}(\mu\text{-PSP})\{\text{Os}_3(^{13}\text{CO})_{10}\}]$  (versus 189.7 ppm for  $1,1-[\text{Os}_3(\text{CO})_{10}(\text{PS})]$ ) that is assigned to the carbonyl *trans* to the sulfur; this doublet is the lowest-field resonance in  $[\{\text{Os}_3(\text{CO})_{11}\}(\mu\text{-PSP})\{\text{Os}_3(^{13}\text{CO})_{10}\}]$  but the second-lowest-field resonance detected in the spectrum of  $1,1-[\text{Os}_3(\text{CO})_{10}(\text{PS})]$ . In both spectra, ten unique resonances could be observed as expected for an unsymmetrical P,S-coordinated cluster with the sulfur in an apical position.

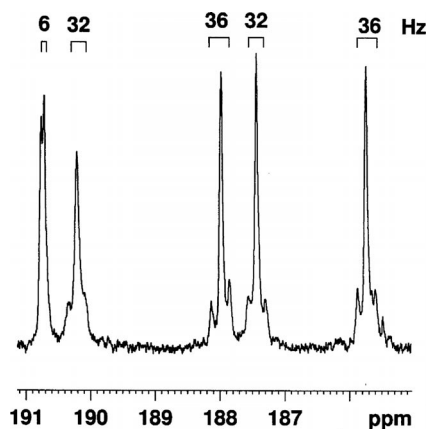


Figure 9. The (partial)  $^{13}\text{C}\{^1\text{H}\}$  NMR spectrum (152.4 MHz,  $\text{CD}_2\text{Cl}_2$ ) of  $1,1-[\{\text{Os}_3(\text{CO})_{11}\}(\mu\text{-PSP})\{\text{Os}_3(^{13}\text{CO})_{10}\}]$  (**4a**) recorded at 213 K; only resonances from the axial carbonyl ligands are shown.

In the low-temperature limiting spectrum of the correspondingly labelled  $1,1-[\{\text{Os}_3(^{13}\text{CO})_{11}\}(\mu\text{-PSP})\{\text{Os}_3(\text{CO})_{10}\}]$  cluster (Figure 10), eleven resonances at  $\delta = 192.4$  (**a/a'**), 191.8 (**a/a'**), 184.5 (**f/f'**), 184.2 (**f/f'**), 183.0 (**c/c'**), 182.8 (**c/c'**), 176.0 (**b**), 175.6 (**h**), 171.6 (**d**), 171.3 (**e**) and 169.2 ppm (**g**) were observed (the bold lettering in parentheses corresponds to the assignment in Figure 3). The resonances at  $\delta = 192.4$ , 191.8, 184.5, 184.2, 183.0 and 182.8 ppm are assigned as the axial carbonyls but occur as pairs. The reason for the presence of multiple resonances is most likely that diastereomeric forms of the complex are formed. As mentioned above, the  $\{\text{Os}_3(\text{CO})_{10}[1,1\text{-PS(P)}]\}$  subunit is a chiral entity in itself; when it is combined with the chirality at the coordinated sulfur atom, diastereomers (two sets of enantiomeric pairs) are formed. The five reso-

nances upfield of  $\delta = 180$  ppm [176.0 (b), 175.6 (h), 171.6 (d), 171.3 (e) and 169.2 ppm (g)] are ascribed to five equatorial carbonyls.

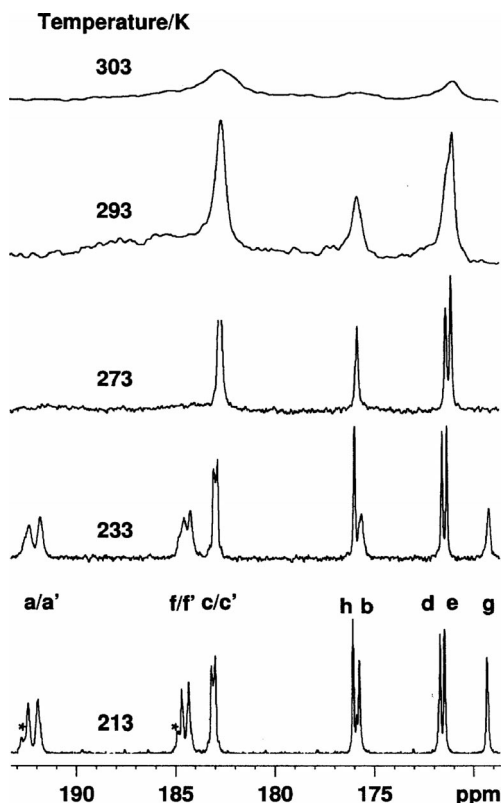
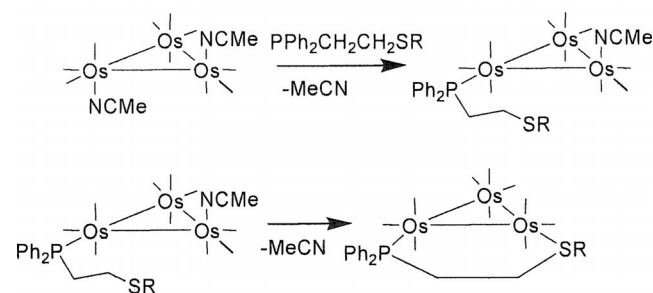


Figure 10. Variable-temperature (VT)  $^{13}\text{C}\{^1\text{H}\}$  NMR spectra of 1,1- $\{[\text{Os}_3(^{13}\text{CO})_{11}](\mu\text{-PSP})\{\text{Os}_3(\text{CO})_{10}\}\}$  (**4a**) (151 MHz,  $\text{CD}_2\text{Cl}_2$ ) in the carbonyl region. The fluxional process is identical to that in **1** (see Figures 2 and 3). However, because the P,S-coordinated  $\{\text{Os}_3(\text{CO})_{10}\}$  subunit is asymmetric, there are 11 independent signals. There is also a minor isomer (marked with \*), which is probably due to a different (minor) diastereomer (see text).

On increasing the temperature to 273 K, the resonances at  $\delta = 183.0$  ppm broaden and merge, probably because the  $\{\text{Os}_3(\text{CO})_{10}\}$  subunit, which is asymmetric (as a consequence of the phosphorus and sulfur coordination), is moving sufficiently fast to average the signals on the NMR spectroscopic timescale. The fluxional process detected for the  $\{\text{Os}_3(\text{CO})_{11}\}$  subunit is identical to that in **1** (see Figures 2 and 3) despite the steric bulk of the second cluster unit in close vicinity of the  $\{\text{Os}_3(\text{CO})_{11}\}$  subunit. The calculated free energy of activation ( $\Delta G^\ddagger$ ) is  $(49.0 \pm 1)$   $\text{kJ mol}^{-1}$  for the merry-go-round process that involves carbonyl ligands **a/a'**, **f,f'**, **b** and **g**, and  $(59.6 \pm 1)$   $\text{kJ mol}^{-1}$  for the process that involves carbonyls **c, c'**, **f, f'**, **d** and **h**. We were unable to observe any intermolecular migration of  $^{13}\text{CO}$  between the  $\{\text{Os}_3(\text{CO})_{11}\}$  and the  $\{\text{Os}_3(\text{CO})_{10}\}$  subunits in any of the enriched samples of **4a**. The above-mentioned NMR spectra are consistent with the calculated structure for the most stable form of  $\{[\text{Os}_3(\text{CO})_{11}](\mu\text{-PSP})\{\text{Os}_3(\text{CO})_{10}\}\}$  [i.e., in which one phosphane moiety and the thioether coordinate in equatorial and axial coordination positions, respectively, so that the ligand chelates one osmium atom of the  $\text{Os}_3(\text{CO})_{10}$  fragment (see Figures 7 and 8)].

### Characterisation of the Metastable Cluster 1,2- $\{[\text{Os}_3(\text{CO})_{11}](\mu\text{-PSP})\{\text{Os}_3(\text{CO})_{10}\}\}$ (**4b**)

In an effort to detect a possible (metastable) 1,2-isomer, the reaction between  $[\text{Os}_3(\text{CO})_{10}(\text{NCMe})_2]$  and  $[\text{Os}_3(\text{CO})_{11}(\text{PSP})]$  was carried out in an NMR tube and monitored by  $^{31}\text{P}\{^1\text{H}\}$  NMR spectroscopy. Immediately upon mixing of the reactants, two singlets of equal intensity were observed at  $\delta = -11.76$  and  $0.5$  ppm. Over a period of 24 h, the singlet at  $0.5$  ppm gradually decreased in intensity with a concomitant increase in the intensity of a new singlet at  $\delta = 39.3$  ppm. The sum of the intensities of the singlets at  $\delta = 0.5$  and  $39.3$  ppm remained constant during the reaction, thus indicating a direct (and quantitative) interconversion/isomerisation. The final  $^{31}\text{P}\{^1\text{H}\}$  NMR spectrum is identical to that of **4a** and the initial spectrum observed upon mixing of the reactants is very similar to that of the metastable cluster 1,2- $[\text{Os}_3(\text{CO})_{10}(\mu\text{-PPh}_2\text{CH}_2\text{CH}_2\text{SMe})]$  (which exhibits a singlet at  $\delta = -0.6$  ppm), thereby suggesting that this spectrum might be attributed to the kinetically favoured isomer **4b**. It is understandable that the formation of **4b** is kinetically favoured; presumably, an intermediate in the reaction of  $[\text{Os}_3(\text{CO})_{11}(\text{PSP})]$  with  $[\text{Os}_3(\text{CO})_{10}(\text{NCMe})_2]$  is the cluster  $\{[\text{Os}_3(\text{CO})_{11}](\mu\text{-PSP})\{\text{Os}_3(\text{CO})_{10}(\text{NCMe})\}\}$  in which the free phosphane moiety of the PSP ligand in  $[\text{Os}_3(\text{CO})_{11}(\text{PSP})]$  (**1**) has replaced one of the two acetonitrile ligands of  $[\text{Os}_3(\text{CO})_{10}(\text{NCMe})_2]$ . As the PSP ligand and the remaining acetonitrile ligand are expected to be coordinated to adjacent atoms, replacement of the second acetonitrile ligand by the thioether moiety leads to the initial formation of **4b** (Scheme 2).



Scheme 2. The reaction of **1** with  $[\text{Os}_3(\text{CO})_{10}(\text{NCMe})_2]$  yields **4b** by stepwise substitution of the acetonitrile ligands.

The dynamic processes and coordination mode(s) of the PSP ligand in **4b** were investigated by variable-temperature (VT)  $^{13}\text{C}$  NMR spectroscopy (Figure 11). The  $^{13}\text{C}$  NMR spectrum in the CO region of the selectively  $^{13}\text{CO}$ -enriched compound 1,2- $\{[\text{Os}_3(\text{CO})_{11}](\mu\text{-PSP})\{\text{Os}_3(^{13}\text{CO})_{10}\}\}$  shows four singlets downfield of  $\delta = 185$  ppm, with intensity ratios 1:1:2:2 at  $\delta = 197.4$ ,  $195.3$ ,  $194.7$  and  $185.2$  ppm. These signals have similar chemical shifts as the resonances assigned to the axial carbonyls in the cluster 1,2- $[\text{Os}_3(\text{CO})_{10}(\mu\text{-PPh}_2\text{CH}_2\text{CH}_2\text{SMe})]$  (196.3, 194.5, 193.5, 193.2 and 184.0 ppm).<sup>[15a]</sup> One difference is that the resonance(s) assigned to the axial carbonyls coordinated to the same metal as the phosphane group are not resolved in **4b**, whereas they

are separated by approximately 0.3 ppm in the spectrum of 1,2-[Os<sub>3</sub>(CO)<sub>10</sub>(μ-PPh<sub>2</sub>CH<sub>2</sub>CH<sub>2</sub>SMe)]. Despite several attempts to generate a clean sample of 1,2-{{Os<sub>3</sub>(CO)<sub>11</sub>}(μ-PSP){Os<sub>3</sub>(<sup>13</sup>CO)<sub>10</sub>}}, additional <sup>13</sup>CO signals due to residual starting materials were identified (Figure 12), namely, [Os<sub>3</sub>(<sup>13</sup>CO)<sub>11</sub>(MeCN)], [Os<sub>3</sub>(<sup>13</sup>CO)<sub>10</sub>(MeCN)<sub>2</sub>] and **1** (see Figure 2).

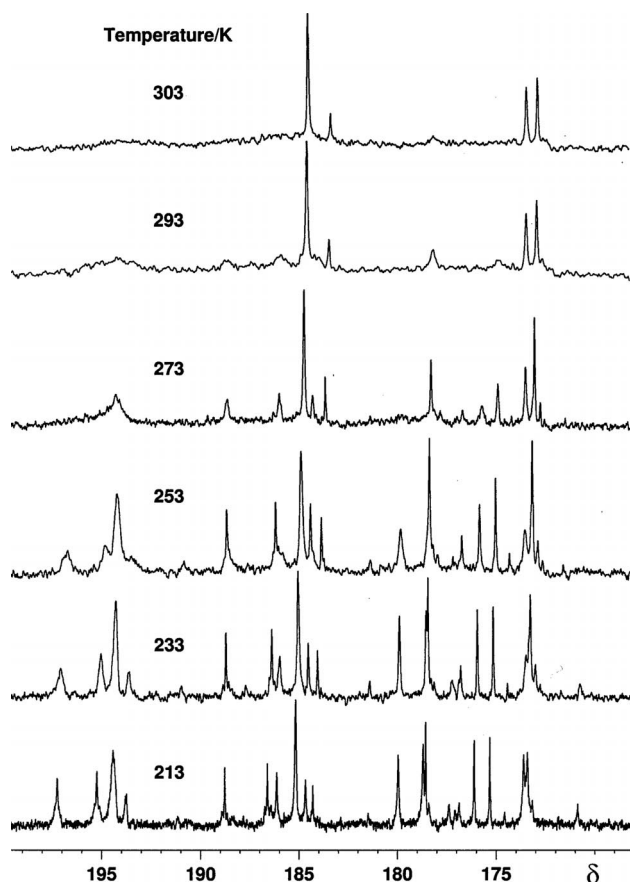


Figure 11. Variable-temperature (VT) <sup>13</sup>C{<sup>1</sup>H} NMR spectra of (metastable) 1,2-{{Os<sub>3</sub>(CO)<sub>11</sub>}(μ-PSP){Os<sub>3</sub>(CO)<sub>10</sub>}} (**4b**) in the carbonyl region (125.7 MHz, CDCl<sub>3</sub>).

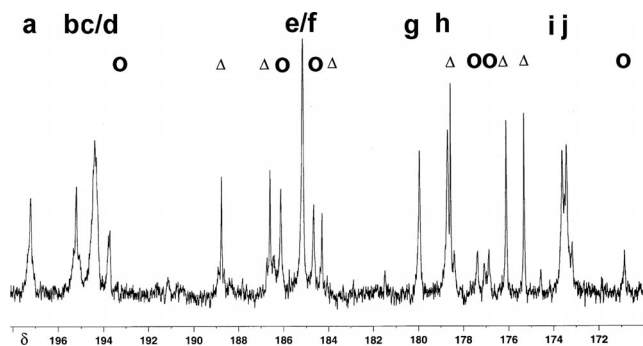


Figure 12. Expansion of the 213 K <sup>13</sup>C{<sup>1</sup>H} spectrum of **4b** showing the assignment of the carbonyl resonances. Resonances due to [Os<sub>3</sub>(CO)<sub>11</sub>(NCMe)] and **1** are marked with Δ and O, respectively.

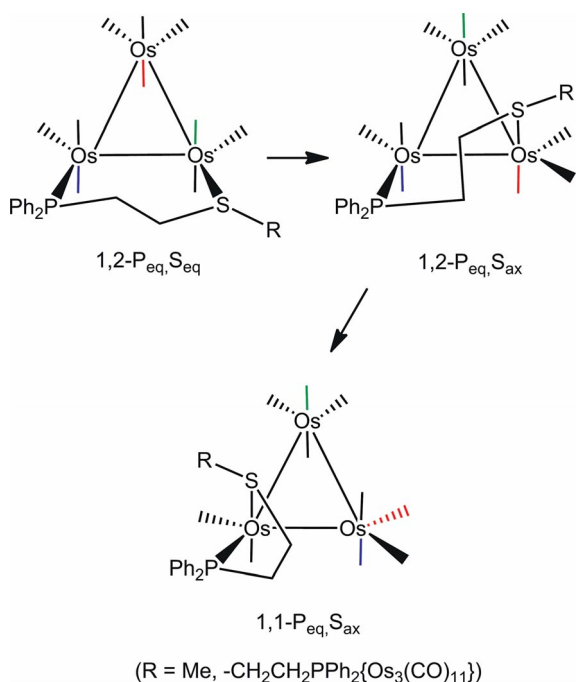
The quality and complexity of the VT <sup>13</sup>C NMR spectra of (selectively enriched) **4b** precluded a full assignment but the similarities in the overall patterns of 1,2-{{Os<sub>3</sub>(CO)<sub>11</sub>}}

(μ-PSP){Os<sub>3</sub>(<sup>13</sup>CO)<sub>10</sub>}} (**4b**) and 1,2-[Os<sub>3</sub>(CO)<sub>10</sub>(μ-PPh<sub>2</sub>CH<sub>2</sub>CH<sub>2</sub>SMe)]<sup>[15a]</sup> are sufficient to conclude that these cluster units are isostructural. Thus, eight resonances were assigned to the {Os<sub>3</sub>(CO)<sub>10</sub>} subunit (Figure 12): the four resonances in 1:1:2:2 relative intensities at δ = 197.2, 195.2, 194.4 and 185.1 ppm represent the axial carbonyl ligands and the four resonances with intensity ratios 1:1:1:1 at δ = 180.0, 178.7, 173.6, and 173.4 ppm represent the equatorial carbonyls. Taken together, the similarities of the IR, <sup>1</sup>H, <sup>31</sup>P{<sup>1</sup>H} and <sup>13</sup>CO{<sup>1</sup>H} data to those previously obtained for 1,2-[Os<sub>3</sub>(CO)<sub>10</sub>(μ-PPh<sub>2</sub>CH<sub>2</sub>CH<sub>2</sub>SMe)] are sufficient to characterise **4b** as having both phosphorus atoms coordinated to the respective metal clusters in equatorial sites, and the <sup>13</sup>C{<sup>1</sup>H} NMR spectroscopic study confirms the equatorial coordination of the sulfur site (see Scheme 3). The structure of cluster **4b** was indirectly confirmed by the fact that **4a** could be obtained in apparent quantitative yield by rearrangement of **4b** in CH<sub>2</sub>Cl<sub>2</sub> over 1–2 days at room temperature.

Two plausible mechanisms exist by which cluster **4b** might isomerise to the more stable isomer **4a**. In the first mechanism, the bound thioether moiety dissociates, a carbonyl ligand migrates to the osmium atom from which the thioether has dissociated and the thioether coordinates at the new vacant coordination site located at the phosphane-substituted osmium centre. In the second mechanism, there is a nondissociative migration of the thioether moiety from its initial locus to the adjacent osmium atom to which the phosphane is coordinated. Coupled with the thioether migration is the subsequent (or concomitant) carbonyl migration (Scheme S1 in the Supporting Information). In the case of the isomerisation of 1,2-[Os<sub>3</sub>(CO)<sub>10</sub>(μ-PPh<sub>2</sub>CH<sub>2</sub>CH<sub>2</sub>SMe)] to 1,1-[Os<sub>3</sub>(CO)<sub>10</sub>(μ-PPh<sub>2</sub>CH<sub>2</sub>CH<sub>2</sub>SMe)]<sup>[15a]</sup> we have found that Δ*S*<sup>‡</sup> is negative, and this allows us to rule out the former process and strongly supports a nondissociative reaction. DFT calculations on the dissociation of the thioether moiety from 1,2-[Os<sub>3</sub>(CO)<sub>10</sub>(μ-PPh<sub>2</sub>PCH<sub>2</sub>CH<sub>2</sub>SMe)] to furnish the coordinatively unsaturated cluster [Os<sub>3</sub>(CO)<sub>10</sub>(κ<sup>P</sup>-Ph<sub>2</sub>PCH<sub>2</sub>CH<sub>2</sub>SMe)] show that the latter species lies 4.5 kcal mol<sup>-1</sup> higher in enthalpy than the rate-limiting step in the nondissociative manifold.<sup>[15c]</sup> The isomerisation of **4b** to **4a** is likely to proceed by a parallel process.

In terms of the nondissociative process, we have shown that isomerisation reactions similar to that discussed above occur in [Os<sub>3</sub>(CO)<sub>10</sub>(P–P)] (P–P = diphosphane) clusters<sup>[35–38]</sup> A computational study<sup>[38]</sup> shows that the favoured mechanism for isomerisation is a merry-go-round mechanism in the equatorial plane of the triangular cluster. An alternative mechanism that was explored but found to be energetically unfavourable involves three consecutive conrotatory permutations of one phosphane moiety and CO groups across an Os–Os vector. The first in-plane migration results in the migration of a phosphane from an equatorial position into an axial position. The isomerisation to the thermodynamically more stable chelated isomer (P<sub>eq</sub>, P<sub>eq</sub>) is then completed through sequential in-plane migration sequences about the same Os–Os vector, with one of the mi-

grations involving a  $\mu_2$ -phosphane moiety. There is a distinct energetic penalty experienced when the phosphane migrates from its preferred equatorial disposition to an axial orientation, thus making this particular manifold noncompetitive relative to the single-step merry-go-round isomerisation process in  $[\text{Os}_3(\text{CO})_{10}(\text{P}-\text{P})]$ . DFT calculations on the dynamical behaviour in our earlier system  $[\text{Os}_3(\text{CO})_{10}(\text{MeSCH}_2\text{CH}_2\text{PPh}_2)]$  reveal a migratory preference for thioether over phosphane migration in the conrotatory in-plane exchange sequences about the Os–Os vector.<sup>[15c]</sup> In fact, the presence of a single thioether moiety in  $[\text{Os}_3(\text{CO})_{10}(\text{MeSCH}_2\text{CH}_2\text{PPh}_2)]$  facilitates consecutive in-plane migrations of the thioether and CO groups such that the merry-go-round process becomes unfavourable. The dynamics for the isomerisation of the thiophosphane moiety in  $[\text{Os}_3(\text{CO})_{10}(\text{MeSCH}_2\text{CH}_2\text{PPh}_2)]$  has been successfully modelled, and Scheme 3 shows the energetically preferred route for the bridge-to-chelate isomerisation of the thiophosphane ligand in  $[\text{Os}_3(\text{CO})_{10}(\text{S}-\text{P})]$ . The migratory process by which **4b** transforms to **4a** is likely to follow the same route exhibited by  $[\text{Os}_3(\text{CO})_{10}(\text{MeSCH}_2\text{CH}_2\text{PPh}_2)]$ .



Scheme 3. Nondissociative mechanism for thioether migration in  $[\text{Os}_3(\text{CO})_{10}(\text{S}-\text{P})]$  clusters; 1,2- $\text{P}_{\text{eq}}, \text{S}_{\text{eq}}$  corresponds to **4b**, 1,1- $\text{P}_{\text{eq}}, \text{S}_{\text{ax}}$  corresponds to **4a**.

## Conclusion

We have found that the mixed-donor ligand PSP, which contains two phosphane and one thioether moieties, readily coordinates to trinuclear osmium compounds. To the best of our knowledge, coordination of the thioether moiety of PSP to a metal has not been observed without prior coordination of the phosphane groups. This is also the case when PSP is coordinated to trinuclear osmium clusters. We have

prepared and structurally characterised five new clusters; in three of these (clusters **1–3**), the PSP ligand coordinates through its phosphane moieties only. Spectroscopic data indicate coordination of the sulfur and the two phosphorus atoms of PSP in **4a**. The selectively enriched samples of **4a**, 1,1- $\{\text{Os}_3(^{13}\text{CO})_{11}\}(\mu\text{-PSP})\{\text{Os}_3(\text{CO})_{10}\}$  and 1,1- $\{\text{Os}_3(\text{CO})_{11}\}(\mu\text{-PSP})\{\text{Os}_3(^{13}\text{CO})_{10}\}$ , were successfully used to determine the coordination modes of the donor atoms of PSP in the cluster. In the  $\{\text{Os}_3(\text{CO})_{10}\}$  unit of compound **4a**, the sulfur is coordinated in an axial position to the same metal atom to which a phosphorus atom is equatorially coordinated. The  $\{\text{Os}_3(\text{CO})_{11}\}$  unit of **4a** has a phosphane group coordinated in an equatorial position. Computational modelling indicates that the observed coordination mode of the PSP ligand is that of lowest energy for the general cluster  $[\{\text{Os}_3(\text{CO})_{11}\}(\mu\text{-PSP})\{\text{Os}_3(\text{CO})_{10}\}]$ . The presence of 11 unique resonances that occur as pairs in 1,1- $\{\text{Os}_3(^{13}\text{CO})_{11}\}(\mu\text{-PSP})\{\text{Os}_3(\text{CO})_{10}\}$  indicates the presence of diastereomers.

The unstable cluster **4b** could be identified in situ when preparing **4a**. The sulfur and a phosphorus coordinate to different osmium atoms of the  $\{\text{Os}_3(\text{CO})_{10}\}$  unit in equatorial positions, whereas the remaining phosphane group in the PSP ligand is equatorially coordinated to the  $\{\text{Os}_3(\text{CO})_{11}\}$  unit. As in the case of **4a**, the unstable cluster **4b** could also be studied by the correspondingly enriched versions 1,2- $\{\text{Os}_3(^{13}\text{CO})_{11}\}(\mu\text{-PSP})\{\text{Os}_3(\text{CO})_{10}\}$  and 1,2- $\{\text{Os}_3(\text{CO})_{11}\}(\mu\text{-PSP})\{\text{Os}_3(^{13}\text{CO})_{10}\}$ . Cluster **4b** slowly converts to **4a**. This type of isomerisation is one of relatively few examples of nondestructive rearrangement of trinuclear clusters with phosphane or thioether ligands in the coordination sphere. Both the cluster framework and the coordinated ligand(s) remain intact throughout the isomerisation process.

## Experimental Section

**General:** All reactions were carried out under an atmosphere of dry nitrogen using standard Schlenk and vacuum-line techniques. The solvents were distilled from appropriate drying agents prior to use. Infrared spectra were recorded as solutions in 0.5 mm NaCl cells with Nicolet 20SXC and Avatar 360 FTIR spectrometers using carbon dioxide as calibrant. Fast-atom bombardment (FAB) mass spectra were obtained with a JEOL SX-102 spectrometer using 3-nitrobenzyl alcohol as matrix and CsI as calibrant. Proton and  $^{31}\text{P}$  NMR spectra were recorded with Varian Unity 300 MHz, Bruker DRX500 500 MHz and Bruker DRX600 600 MHz spectrometers. Routine separations of products were performed by thin-layer chromatography using commercially prepared glass plates, pre-coated with 0.25 mm Merck Silica gel 60. Column chromatography was carried out using silica gel (Merck Silica gel 60, 0.040–0.063 mm, 230–400 mesh, ASTM) columns, initially packed in  $\text{CH}_2\text{Cl}_2$ . The starting materials,  $[\text{Os}_3(\text{CO})_{11}(\text{NCMe})]$  and  $[\text{Os}_3(\text{CO})_{10}(\text{NCMe})_2]$ , were synthesised according to literature methods.<sup>[18]</sup>

**Preparation of Divinyl Sulfide:** Divinyl sulfide was prepared according to a published method.<sup>[40]</sup> In a typical reaction, potassium hydroxide (20 g, 0.36 mol) and bis(2-hydroxyethyl)sulfide (20 mL, 0.134 mol) were mixed in a distillation apparatus. The mixture was

carefully heated under a nitrogen stream until the reaction started (ca. 150–200 °C). When the temperature exceeded approximately 150 °C, water and product were formed and distilled. The water was separated from the product in an extraction flask. The product was then distilled at 760 Torr and the fraction collected at 92–93 °C was collected. The product was stored over molecular sieves (12 Å) in a freezer. <sup>1</sup>H NMR (CDCl<sub>3</sub>, 300 MHz, 298 K): δ = 5.31 (d, <sup>3</sup>J<sub>H,H</sub> = 9 Hz, 2 H *trans* to S), 5.32 (d, <sup>3</sup>J<sub>H,H</sub> = 17 Hz, 2 H *cis* to S), 6.41 (dd, <sup>3</sup>J<sub>H,H-*cis*</sub> = 9 Hz; <sup>3</sup>J<sub>H,H-*trans*</sub> = 17 Hz, 2 H, SCH) ppm.

**Preparation of PSP:** The reagents divinyl sulfide (909 mg, 10.5 mmol), diphenylphosphane (3.92 g, 21.1 mmol) and azobisisobutyronitrile (AIBN, 0.1 g, 0.169 mmol) were heated in a Schlenk tube at approximately 120 °C under a nitrogen flow for 1 h and then dried under reduced pressure for 1 h at 120 °C. The product was filtered through a silica column using dichloromethane as eluent. Separation by TLC, using a CHCl<sub>3</sub>/hexane mixture (1:4 v/v) as eluent, yielded one fraction. The last part of the eluate was slightly contaminated and was therefore discarded. The residual oil obtained after removal of solvent under reduced pressure was triturated with hexane until a white crystalline solid was formed. Yield: 2.35 g (49%), m.p. 58–60 °C. <sup>1</sup>H NMR (CDCl<sub>3</sub>, 300 MHz): δ = 2.27 (m, 4 H, CH<sub>2</sub>S), 2.58 (m, 4 H, PCH<sub>2</sub>), 7.3–7.5 (m, 20 H) ppm. <sup>31</sup>P{<sup>1</sup>H} NMR (H<sub>3</sub>PO<sub>4</sub>: δ = 0 ppm, downfield positive): δ = –16.0 (s, 2 P) ppm. <sup>13</sup>C{<sup>1</sup>H} NMR (CDCl<sub>3</sub>, 150.9 MHz): δ = 27.98 (d, <sup>2</sup>J<sub>C,P</sub> = 21.3 Hz, 2 C, CH<sub>2</sub>S), 28.31 (d, <sup>1</sup>J<sub>C,P</sub> = 14.89 Hz, 2 C, PCH<sub>2</sub>), 128.38 (d, <sup>3</sup>J<sub>C,P</sub> = 6.64 Hz, 8 C, *meta*-C, Ph), 128.62 (s, 4 C, *para*-C, Ph), 132.62 (d, <sup>2</sup>J<sub>C,P</sub> = 18.6 Hz, 8 C, *ortho*-C, Ph), 137.66 (d, <sup>1</sup>J<sub>C,P</sub> = 13.1 Hz, 4 C, *ipso*-C, Ph) ppm.

**Synthesis of [Os<sub>3</sub>(CO)<sub>11</sub>(PSP)] (1):** In a typical reaction, [Os<sub>3</sub>(CO)<sub>11</sub>(NCMe)] (100 mg, 0.109 mmol) was dissolved in dichloromethane (10 mL). This solution was added dropwise over a period of 20 min to a stirred solution of PSP (100 mg, 0.218 mmol) in CH<sub>2</sub>Cl<sub>2</sub> (20 mL). The solution was stirred at room temperature until no ν<sub>CO</sub> resonances due to the starting material could be detected (1.5 h). The solvent was removed under vacuum and the crude product was separated by thin-layer chromatography using a 1:1 hexane/CH<sub>2</sub>Cl<sub>2</sub> mixture as eluent. Three bands were recovered, in order of decreasing R<sub>f</sub>: [(Os<sub>3</sub>(CO)<sub>11</sub>)<sub>2</sub>(μ-PSP)] (2), yellow, 30 mg (0.013 mmol); [Os<sub>3</sub>(CO)<sub>11</sub>(PSP)] (1), yellow, 58 mg (0.043 mmol) followed by 5 mg of one, as yet, uncharacterised, yellow fraction. IR (ν<sub>CO</sub>; hexane):  $\tilde{\nu}$  = 2108 (m), 2056 (s), 2034 (w), 2019 (vs), 2002 (vw), 1991 (mw), 1980 [mw(b)] cm<sup>-1</sup>. <sup>1</sup>H NMR (in CDCl<sub>3</sub>): δ = 2.9 (m, 2 H), 2.5 (m, 2 H), 2.3 (m, 2 H), 2.1 (m, 2 H), 7.3–7.5 (m, 20 H) ppm. <sup>31</sup>P{<sup>1</sup>H} NMR (H<sub>3</sub>PO<sub>4</sub>: δ = 0 ppm, downfield positive): δ = –10.9 (s, 1 P), –16.6 (s, 1 P) ppm. <sup>13</sup>C{<sup>1</sup>H} NMR (126 MHz, CDCl<sub>3</sub>, 213 K): δ = 192.4 (d, <sup>2</sup>J<sub>PC</sub> = 8.0 Hz, 1 C), 184.7 (s, 1 C), 183.3 (s, 1 C), 176.1 (s, 1 C), 175.9 (s, 1 C), 172.1 (s, 1 C), 171.8 (s, 1 C), 169.5 (s, 1 C) ppm. Calcd. for 1: C 35.0, H 2.10, P 4.60, S 2.40, N 0; found C 34.95, H 2.15, P 4.45, S 2.30, N <0.2.

**Synthesis of [(Os<sub>3</sub>(CO)<sub>11</sub>)<sub>2</sub>(μ-PSP)] (2):** In a typical reaction, [Os<sub>3</sub>(CO)<sub>11</sub>(NCMe)] (208 mg, 0.226 mmol) and PSP (52 mg, 0.113 mmol) were dissolved in CH<sub>2</sub>Cl<sub>2</sub> (30 mL) and stirred at room temperature until no ν<sub>CO</sub> resonances due to the starting material could be detected (2 h). The solvent was then removed under vacuum at 40 °C. The crude product was separated by TLC using a hexane/CH<sub>2</sub>Cl<sub>2</sub> mixture (1:1 v/v) as eluent and yielded two bands; in order of decreasing R<sub>f</sub>: [(Os<sub>3</sub>(CO)<sub>11</sub>)<sub>2</sub>(μ-PSP)], yellow, 150 mg (0.067 mmol); [Os<sub>3</sub>(CO)<sub>11</sub>(PSP)], orange 5 mg (0.0037 mmol). IR [ν(CO); in hexane]:  $\tilde{\nu}$  = 2107 (m), 2054 (s), 2033 (w), 2020 (vs), 2002 (vw), 1990 [mw (b)], 1977 [w (b)] cm<sup>-1</sup>. <sup>1</sup>H NMR (CDCl<sub>3</sub>): δ = 2.8 (m, 2 H), 2.3 (m, 2 H), 7.2–7.5 (m, 20 H) ppm. <sup>31</sup>P{<sup>1</sup>H} NMR (H<sub>3</sub>PO<sub>4</sub>: δ = 0 ppm, downfield positive): δ = –10.7 (s, 2 P) ppm.

### Synthesis of [Os<sub>3</sub>(CO)<sub>10</sub>(μ-PSP)] (3)

**Method I:** [Os<sub>3</sub>(CO)<sub>10</sub>(NCMe)<sub>2</sub>] (93 mg, 0.150 mmol) and PSP (93 mg, 0.100 mmol) were dissolved in CHCl<sub>3</sub> (30 mL). The solution was heated at reflux for 3 h. The solvent was removed under reduced pressure at 40 °C and the crude product was separated by thin-layer chromatography using a 3:2 hexane/CH<sub>2</sub>Cl<sub>2</sub> mixture as eluent. Three bands were isolated; in order of decreasing R<sub>f</sub>: [Os<sub>3</sub>(CO)<sub>10</sub>(μ-PSP)] (3), red, 21 mg (0.016 mmol) followed by two, as yet, uncharacterised, yellow fractions.

**Method II:** Me<sub>3</sub>NO (2.95 mg, 0.039 mmol) was dissolved in CH<sub>2</sub>Cl<sub>2</sub> (20 mL). This solution was transferred dropwise over 20 min to a stirred solution of [Os<sub>3</sub>(CO)<sub>11</sub>(η<sup>1</sup>-PSP)] (50 mg, 0.037 mmol) in CH<sub>2</sub>Cl<sub>2</sub>. The solution was stirred at room temperature for 20 h. The solvent was removed under reduced pressure and the crude product was separated by thin-layer chromatography using a 3:2 hexane/CH<sub>2</sub>Cl<sub>2</sub> mixture as eluent. Four bands were recovered, in order of decreasing R<sub>f</sub>: [Os<sub>3</sub>(CO)<sub>10</sub>(μ-PSP)] (3), red, 7 mg (0.0053 mmol) followed by three, as yet unidentified, yellow fractions. For 3: IR [ν(CO); in hexane]:  $\tilde{\nu}$  = 2085 (m–s), 2020 (m), 2011 (s), 2002 (vs), 1976 (vw), 1957 (w) cm<sup>-1</sup>. <sup>1</sup>H NMR (CDCl<sub>3</sub>): δ = 3.0 (m, 2 H), 2.2 (m, 2 H) 7.0–7.8 (m, 20 H) ppm. <sup>31</sup>P{<sup>1</sup>H} NMR (H<sub>3</sub>PO<sub>4</sub>: δ = 0 ppm, downfield positive): δ = –4.3 (s, 2 P) ppm.

### Synthesis of 1,1-{Os<sub>3</sub>(CO)<sub>11</sub>}(μ-PSP){Os<sub>3</sub>(CO)<sub>10</sub>} (4a)

**Method I:** [Os<sub>3</sub>(CO)<sub>11</sub>(PSP)] (30 mg, 0.022 mmol) was dissolved in CH<sub>2</sub>Cl<sub>2</sub> (5 mL), which was added dropwise over a period of 10 min to a stirred solution of [Os<sub>3</sub>(CO)<sub>10</sub>(NCMe)<sub>2</sub>] (42 mg, 0.044 mmol) in CH<sub>2</sub>Cl<sub>2</sub> (15 mL). The solution was stirred at room temperature for 2 h. The solvent was then removed under reduced pressure at 40 °C. The crude product was separated by TLC eluent (hexane/CH<sub>2</sub>Cl<sub>2</sub>, 3:2 v/v) to yield orange [Os<sub>6</sub>(CO)<sub>21</sub>(PSP)] (4a) 50%.

**Method II:** Me<sub>3</sub>NO (1.31 mg, 0.0174 mmol) was dissolved in a 1:1 CH<sub>2</sub>Cl<sub>2</sub>/MeCN solution (2.5 mL). This solution was added dropwise over a period of 20 min to a solution of [(Os<sub>3</sub>(CO)<sub>11</sub>)<sub>2</sub>(μ-PSP)] (38 mg, 0.0171 mmol). The mixture was stirred overnight and the solvent was removed under reduced pressure at 40 °C. Separation by TLC, eluent hexane/CH<sub>2</sub>Cl<sub>2</sub> (3:2 v/v), yielded orange [Os<sub>6</sub>(CO)<sub>21</sub>(PSP)] in 30% yield. For 4a: IR [ν(CO); in hexane]:  $\tilde{\nu}$  = 2109 (m), 2088 (m), 2071 (w), 2057 (s), 2039 (s), 2021 (vs), 2013 (ms), 1993 (s), 1982 (m) cm<sup>-1</sup>. <sup>1</sup>H NMR (CDCl<sub>3</sub>): δ = 2.9 (m, 2 H), 2.8 (m, 2 H), 2.6 (m, 2 H), 2.4 (m, 2 H), 1.8 (m) ppm. <sup>31</sup>P{<sup>1</sup>H} NMR (H<sub>3</sub>PO<sub>4</sub>: δ = 0 ppm): δ = 39.3 (s, 1 P), –11.8 (s, 1 P) ppm. <sup>13</sup>C{<sup>1</sup>H} NMR (CD<sub>2</sub>Cl<sub>2</sub>, 125.8 MHz, 213 K) of 1,1-{Os<sub>3</sub>(<sup>13</sup>CO)<sub>10</sub>}(μ-PSP){Os<sub>3</sub>(CO)<sub>11</sub>}: δ = 190.7 (d, <sup>2</sup>J<sub>C,P</sub> = 6 Hz, 1 C), 190.2 (<sup>2</sup>J<sub>C,C</sub> = 32 Hz, 1 C), 187.9 (t, <sup>2</sup>J<sub>C,C</sub> = 36 Hz, 1 C), 187.4 (t, <sup>2</sup>J<sub>C,C</sub> = 32 Hz, 1 C), 185.7 (t, <sup>2</sup>J<sub>C,C</sub> = 36 Hz, 1 C), 181.1 (s, 1 C), 178.3 (s, 1 C), 176.7 (s, 1 C), 174.2 (s, 1 C), 172.9 (s, 1 C) ppm. <sup>13</sup>C{<sup>1</sup>H} NMR (CDCl<sub>3</sub>, 150.8 MHz, 213 K) of 1,1-{Os<sub>3</sub>(CO)<sub>10</sub>}(μ-PSP){Os<sub>3</sub>(<sup>13</sup>CO)<sub>11</sub>}: δ = 192.4 (s, 1 C), 191.8 (s, 1 C), 184.5 (s, 1 C), 184.2 (s, 1 C), 183.0 (s, 1 C), 182.8 (s, 1 C), 176.0 (s, 1 C), 175.6 (s, 1 C), 171.6 (s, 1 C), 171.3 (s, 1 C) 169.2 (s, 1 C) ppm.

**Synthesis of 1,2-{Os<sub>3</sub>(CO)<sub>11</sub>}(μ-PSP){Os<sub>3</sub>(CO)<sub>10</sub>} (4b):** The compound 1,2-{Os<sub>3</sub>(CO)<sub>11</sub>}(μ-PSP){Os<sub>3</sub>(CO)<sub>10</sub>} was identified as an intermediate in the preparation of 4a. An amount of [Os<sub>3</sub>(CO)<sub>11</sub>(PSP)] (30 mg, 0.022 mmol) was dissolved in CH<sub>2</sub>Cl<sub>2</sub> (5 mL), which was added dropwise over a period of 10 min to a stirred solution of [Os<sub>3</sub>(CO)<sub>10</sub>(NCMe)<sub>2</sub>] (42 mg, 0.044 mmol) in CH<sub>2</sub>Cl<sub>2</sub> (15 mL). The solution was stirred at room temperature for 15 min. The solvent was then removed under reduced pressure to yield orange 1,2-[Os<sub>6</sub>(CO)<sub>21</sub>(PSP)] (50%). <sup>31</sup>P{<sup>1</sup>H} NMR (CDCl<sub>3</sub>, 303 K): δ = –11.76 (s, 1 P), 0.5 (s, 1 P) ppm. <sup>13</sup>C{<sup>1</sup>H} NMR (CDCl<sub>3</sub>, 213 K) of 1,2-{Os<sub>3</sub>(CO)<sub>11</sub>}(μ-PSP){Os<sub>3</sub>(<sup>13</sup>CO)<sub>10</sub>}: δ =

197.2 (s, 1 C), 195.2 (s, 1 C), 194.4 (s, 2 C), 185.1 (s, 2 C), 180.0 (s, 1 C), 178.7 (s, 1 C), 173.6 (s, 1 C), 173.4 (s, 1 C), 174.0 (s, 1 C), 172.1 (s, 1 C) ppm.

**Computational Methodology:** The DFT calculations reported here were performed with the Gaussian 09 package of programs.<sup>[41]</sup> The calculations were carried out with the B3LYP functional, which utilizes the Becke three-parameter exchange functional (B3)<sup>[42]</sup> combined with the correlation functional of Lee, Yang and Parr (LYP).<sup>[43]</sup> The osmium atoms were described by Stuttgart–Dresden effective core potentials (ecp) and the SDD basis set, whereas the 6-31G(d') basis set, as implemented in the Gaussian 09 program package, was employed for the remaining atoms. The geometry-optimized structures reported here represent minima based on zero imaginary frequencies (positive eigenvalues), as established by frequency calculations using the analytical Hessian. The geometry-optimised structures have been drawn with the JIMP2 molecular visualisation and manipulation program.<sup>[44]</sup>

**Crystallography:** Yellow crystals of **2** were grown by slow evaporation from a dichloromethane/*n*-hexane solution at 4 °C. Cluster **3** was crystallised as bright orange plates from a dichloromethane solution at –10 °C. Crystal data and experimental details of the data collections and structure refinements for **2** and **3** are summarised in Table 3.

**X-ray Data Collection and Structure Determination of 2:** The diffraction experiments were carried out at room temperature with a fully automated Enraf–Nonius CAD-4 diffractometer using graphite-monochromated Mo- $K_{\alpha}$  radiation. The unit-cell parameters were determined by a least-squares fitting procedure using 25 reflections. Data were corrected for Lorentz and polarisation effects. A decay (32%) and an empirical absorption correction using the azimuthal scan method were applied.<sup>[45]</sup> The positions of the metal atoms were found by direct methods using the SHELXS 97 program.<sup>[46]</sup> Least-squares refinements and Fourier-difference syntheses revealed all the remaining non-hydrogen atoms and the presence of some peaks attributable to a highly disordered CH<sub>2</sub>Cl<sub>2</sub> molecule. The phenyl rings were treated like ideal hexagons (length C–C:

1.39 Å, angle C–C–C: 120°). The phenyl and methylene hydrogen atoms were added in calculated positions ( $d_{C-H} = 0.96$  Å). The final refinement on  $F^2$  proceeded by full-matrix least-squares calculations (SHELXL 97)<sup>[47]</sup> using anisotropic thermal parameters for all the non-hydrogen atoms. The phenyl and methylene hydrogen atoms were assigned an isotropic thermal parameter 1.2 times  $U_{eq}$  of the carbon atoms to which they were attached.

**X-ray Data Collection and Structure Determination of 3:** The X-ray intensity data for **3** were measured with a Bruker AXS SMART 2000 diffractometer, equipped with a CCD detector, using Mo- $K_{\alpha}$  radiation ( $\lambda = 0.71073$  Å) at room temperature. Cell dimensions and the orientation matrix were initially determined from least-squares refinement on reflections measured in three sets of 20 exposures collected in three different  $\omega$  regions and eventually refined against 5905 reflections. A full sphere of reciprocal space was scanned by 0.3°  $\omega$  steps. Intensity decay was monitored by recollecting the initial 50 frames at the end of the data collection and analysing the duplicate reflections. The collected frames were processed for integration by using the SAINT program and an empirical absorption correction was applied using SADABS<sup>[48]</sup> on the basis of the Laue symmetry of the reciprocal space. The structure was solved by direct methods (SIR 97)<sup>[49]</sup> and subsequent Fourier syntheses and refined by full-matrix least-squares on  $F^2$  (SHELXTL)<sup>[50]</sup> using anisotropic thermal parameters for all non-hydrogen atoms. The phenyl and methylene hydrogen atoms were added in calculated positions ( $d_{C-H} = 0.96$  Å) and assigned an isotropic thermal parameter 1.5 and 1.2 times  $U_{eq}$  of the carbon atoms to which they were attached. Crystal data and other experimental details for **2** and **3** are reported in Table 3.

CCDC-821723 (for **2**) and -821724 (for **3**) contain the supplementary crystallographic data for this paper. These data can be obtained free of charge from The Cambridge Crystallographic Data Centre via [www.ccdc.cam.ac.uk/data\\_request/cif](http://www.ccdc.cam.ac.uk/data_request/cif).

**Supporting Information** (see footnote on the first page of this article): Description of alternative crystal form for **3**. Schematic depiction of dissociative and nondissociative pathways for isomerisation

Table 3. Crystal data and experimental details for **2** and **3**.

Compound	<b>2</b>	<b>3</b>
Formula	C <sub>50</sub> H <sub>28</sub> O <sub>22</sub> Os <sub>6</sub> P <sub>2</sub> S·0.6CH <sub>2</sub> Cl <sub>2</sub>	CH <sub>38</sub> H <sub>28</sub> O <sub>10</sub> Os <sub>3</sub> P <sub>2</sub> S·0.9CH <sub>2</sub> Cl <sub>2</sub>
$M_r$	2265.88	1387.34
$T$ [K]	293(2)	293(2)
$\lambda$ [Å]	0.71073	0.71073
Crystal symmetry	monoclinic	orthorhombic
Space group	$P2_1/a$ (no. 14)	$P2_12_12_1$ (no.19)
$a$ [Å]	15.694(8)	11.824(1)
$b$ [Å]	13.804(5)	16.945(1)
$c$ [Å]	28.955(9)	21.635(1)
$\beta$ (°)	99.98(3)	90
$V$ [Å <sup>3</sup> ]	6178(4)	4334.7(5)
$Z$	4	4
$D_{\text{calcd.}}$ [Mg m <sup>-3</sup> ]	2.4360	2.126
$\mu$ (Mo- $K_{\alpha}$ ) [mm <sup>-1</sup> ]	12.502	9.061
$F(000)$	4120	2595
Crystal size [mm]	0.07 × 0.12 × 0.20	0.15 × 0.30 × 0.42
$\theta$ limits [°]	2–25	1.5–30
Reflections collected	10731 [ $\pm h$ , $+k$ , $+l$ ]	59329 [ $\pm h$ , $\pm k$ , $\pm l$ ]
Unique observed reflections	10722 [ $R(\text{int})$ 0.00]	10518 [ $R(\text{int})$ 0.07]
$[F_o > 4\sigma(F_o)]$		
GoF on $F^2$	1.051	0.90
$R_1$ ( $F$ ) <sup>[a]</sup> , $wR_2$ ( $F^2$ ) <sup>[b]</sup>	0.0309, 0.0636	0.0264, 0.0503
Largest diff. peak and hole [e Å <sup>-3</sup> ]	1.68 and –1.40	1.12 and –0.97

[a]  $R_1 = \sum ||F_o| - |F_c|| / \sum |F_o|$ . [b]  $wR_2 = [\sum w(F_o^2 - F_c^2)^2 / \sum w(F_o^2)^2]^{1/2}$  in which  $w = 1/[\sigma^2(F_o^2) + (aP)^2 + bP]$  in which  $P = (F_o^2 + 2F_c^2)/3$ .

of cluster **4b** to **4a**. Atomic coordinates and energies for the geometry-optimised structures of clusters **4a** and **4b**. These materials are available upon request from M. G. R.

## Acknowledgments

M. M. wishes to thank the University of Bologna and Ministero dell'Università e della Ricerca (MIUR) (PRIN 2008) for financial support. M. G. R. acknowledges support from the Robert A. Welch Foundation (grant number B-1093-MGR) and National Science Foundation (NSF) (CHE-0741936). The authors thank Prof. Carlaxel Andersson for a generous gift of PSP, Prof. Silvio Aime for the use of the DRX600 NMR spectrometer in Ivrea, Italy and Dr. Karl-Erik Bergquist for the use of the DRX500 NMR spectrometer at Lund University. The authors thank Dr. Håkan Carlsson for useful suggestions for the synthesis of PSP. The authors also thank Prof. Michael B. Hall (TAMU) for providing us a copy of his JIMP2 program, which was used to prepare the geometry-optimised structures reported here.

- [1] a) M. P. Brown, P. A. Bolby, M. M. Harding, A. J. Mathews, A. K. Smith, *J. Chem. Soc., Dalton Trans.* **1993**, 1671; b) A. W. Coleman, D. F. Jones, P. H. Dixneuf, C. Brisson, J. J. Bonnet, G. Lavigne, *Inorg. Chem.* **1984**, *23*, 952.
- [2] B. F. G. Johnson, J. Lewis, M. Monari, D. Braga, F. Grepioni, C. Gradella, *J. Chem. Soc., Dalton Trans.* **1990**, 2863.
- [3] a) S. Cartwright, J. A. Clucas, R. H. Dawson, D. F. Foster, M. M. Harding, A. K. Smith, *J. Organomet. Chem.* **1986**, *302*, 403; b) E. R. Corey, L. F. Dahl, *Inorg. Chem.* **1962**, *1*, 521; c) J. A. Clucas, D. F. Foster, M. M. Harding, A. K. Smith, *J. Chem. Soc., Chem. Commun.* **1984**, 949.
- [4] B. F. G. Johnson, *J. Chem. Soc., Chem. Commun.* **1976**, 211.
- [5] D. F. Foster, J. Harrison, B. S. Nicholls, A. K. Smith, *J. Organomet. Chem.* **1985**, *295*, 99.
- [6] J. A. Clucas, M. M. Harding, A. K. Smith, *J. Chem. Soc., Chem. Commun.* **1985**, 1280.
- [7] S. R. Hodge, B. F. G. Johnson, J. Lewis, P. R. Raithby, *J. Chem. Soc., Dalton Trans.* **1987**, 931.
- [8] a) A. J. Deeming, S. Donovan-Mtunzi, S. E. Kabir, *J. Organomet. Chem.* **1984**, *276*, C65; b) A. J. Deeming, K. I. Hardcastle, S. E. Kabir, *J. Chem. Soc., Dalton Trans.* **1988**, 827; c) A. J. Deeming, S. E. Kabir, *J. Organomet. Chem.* **1988**, *340*, 359.
- [9] S. E. Kabir, A. Miah, L. Nesa, K. Uddin, K. I. Hardcastle, E. Rosenberg, A. J. Deeming, *J. Organomet. Chem.* **1995**, *492*, 41.
- [10] P. E. Garrou, *Chem. Rev.* **1981**, *81*, 229.
- [11] E. Hauptman, P. J. Fagan, W. Marshall, *Organometallics* **1999**, *18*, 2061, and references therein.
- [12] J. R. Dilworth, N. Wheatley, *Coord. Chem. Rev.* **2000**, *199*, 89.
- [13] A. J. Deeming, S. N. Jayasuriya, A. J. Arce, Y. De Sanctis, *Organometallics* **1996**, *15*, 786.
- [14] a) J. D. King, M. Monari, E. Nordlander, *J. Organomet. Chem.* **1999**, *573*, 272; b) S. P. Tunik, I. O. Koshevoy, A. J. Poe, D. H. Farrar, E. Nordlander, T. A. Pakkanen, M. Haukka, *Dalton Trans.* **2003**, 2457; c) N. K. Kiriakidou Kazemifar, M. J. Stchedroff, M. A. Mottalib, S. Selva, M. Monari, E. Nordlander, *Eur. J. Inorg. Chem.* **2006**, 2058; d) M. A. Mottalib, S. E. Kabir, D. A. Tocher, A. J. Deeming, E. Nordlander, *J. Organomet. Chem.* **2007**, *692*, 5007; e) M. N. Uddin, N. Begum, M. R. Hassan, G. Hogarth, S. E. Kabir, M. Arzu Miah, E. Nordlander, D. A. Tocher, *Dalton Trans.* **2008**, 6219; f) M. N. Uddin, M. A. Mottalib, N. Begum, S. Ghosh, A. K. Raha, D. T. Haworth, S. V. Lindeman, T. A. Siddiquee, D. W. Bennett, G. Hogarth, E. Nordlander, S. E. Kabir, *Organometallics* **2009**, *28*, 1514; g) S. Ghosh, A. K. Das, N. Begum, D. T. Haworth, S. V. Lindeman, J. F. Gardinier, T. A. Siddiquee, D. W. Bennett, E. Nordlander, G. Hogarth, S. E. Kabir, *Inorg. Chim. Acta* **2009**, *362*, 5175; h) S. Ghosh, G. Hogarth, D. A. Tocher, E. Nordlander, S. E. Kabir, *Inorg. Chim. Acta* **2010**, *363*, 1611.
- [15] a) R. Persson, M. Monari, R. Gobetto, A. Russo, S. Aime, M. J. Calhorda, E. Nordlander, *Organometallics* **2001**, *20*, 4150; b) R. Persson, M. J. Stchedroff, B. Uebersezig, R. Gobetto, J. W. Steed, P. D. Prince, M. Monari, E. Nordlander, *Organometallics* **2010**, *29*, 2223; c) D. A. Hrovat, E. Nordlander, M. G. Richmond, *Organometallics* **2012**, *31*, 6608.
- [16] a) G. Schwarzenbach, *Chem. Zvesti* **1965**, *19*, 200; b) B. D. Steffey, A. Miedaner, M. L. Maciejewski-Farmer, *Organometallics* **1994**, *13*, 4844; c) G. Degischer, G. Schwarzenbach, *Helv. Chim. Acta* **1966**, *49*, 1927; d) G. Degischer, Ph. D. Thesis, ETH, Zürich, **1968**; e) L. Fälth, Ph. D. Thesis, Lund University, **1976**; f) G. I. Bertinsson, Ph. D. Thesis, Lund University, **1982**; g) A. Cassel, Ph. D. Thesis, Lund University, **1979**.
- [17] P. A. Dawson, B. F. G. Johnson, J. Lewis, J. Puga, P. R. Raithby, M. J. Rosales, *J. Chem. Soc., Dalton Trans.* **1982**, 233.
- [18] B. F. G. Johnson, J. Lewis, D. A. Pippard, *J. Chem. Soc., Dalton Trans.* **1981**, 407.
- [19] a) D. H. Brown, R. J. Cross, D. J. Millington, *J. Chem. Soc., Dalton Trans.* **1976**, 334; b) D. L. DuBois, W. H. Myers, D. W. Meek, *J. Chem. Soc., Dalton Trans.* **1975**, 101.
- [20] A. J. Deeming, S. Donovan-Mtunzi, S. E. Kabir, *J. Organomet. Chem.* **1987**, *333*, 253.
- [21] M. J. Stchedroff, S. Aime, R. Gobetto, L. Salassa, E. Nordlander, *Magn. Res. Chem.* **2002**, *40*, 107.
- [22] B. F. G. Johnson, B. E. Reichert, K. T. Schorpp, *J. Chem. Soc., Dalton Trans.* **1976**, 1403.
- [23] R. F. Alex, R. K. Pomeroy, *Organometallics* **1987**, *6*, 2437.
- [24] K. Biradha, V. M. Hansen, W. K. Leong, R. K. Pomeroy, J. Zaworotko, *J. Cluster Sci.* **2000**, *11*, 285, and references therein.
- [25] A. J. Deeming, in: *Comprehensive Organometallic Chemistry II* (Eds.: E. W. Abel, F. G. A. Stone, G. Wilkinson), Elsevier, Oxford, UK, **1995**, vol. 7, pp. 683–746.
- [26] M. I. Bruce, T. W. Hambley, B. K. Nicholson, M. R. Snow, *J. Organomet. Chem.* **1982**, *235*, 83.
- [27] S. G. Ang, X. Zhong, H. G. Ang, *J. Chem. Soc., Dalton Trans.* **2001**, 1151.
- [28] S. G. Ang, X. Zhong, H. G. Ang, *Inorg. Chem.* **2002**, *41*, 3791.
- [29] a) M. I. Bruce, M. J. Liddell, C. A. Hughes, B. W. Skelton, A. H. White, *J. Organomet. Chem.* **1988**, *347*, 157; b) M. I. Bruce, J. M. Addick, C. A. Hughes, J. A. Patrick, B. W. Skelton, A. H. White, *J. Organomet. Chem.* **1988**, *347*, 181; c) M. I. Bruce, M. J. Liddell, O. Bin Shawkataly, C. A. Hughes, B. W. Skelton, A. H. White, *J. Organomet. Chem.* **1988**, *347*, 207.
- [30] M. R. Churchill, B. G. DeBoer, *Inorg. Chem.* **1977**, *16*, 878.
- [31] a) A. J. Deeming, S. Donovan-Mtunzi, K. I. Hardcastle, S. E. Kabir, K. Henrick, M. J. McPartlin, *J. Chem. Soc., Dalton Trans.* **1988**, 579; b) S. E. Kabir, A. Miah, L. Nesa, K. Uddin, K. I. Hardcastle, E. Rosenberg, A. J. Deeming, *J. Organomet. Chem.* **1995**, *492*, 41; c) K. A. Azam, M. B. Hursthouse, S. E. Kabir, K. M. Abdul Malik, A. Mottalib, *J. Chem. Crystallogr.* **1999**, *29*, 813.
- [32] R. E. Benfield, B. F. G. Johnson, *J. Chem. Soc., Dalton Trans.* **1980**, 1743.
- [33] M. R. Churchill, F. J. Hollander, J. P. Hutchinson, *Inorg. Chem.* **1977**, *16*, 2655.
- [34] J. W. Lauher, *J. Am. Chem. Soc.* **1986**, *108*, 1521.
- [35] W. H. Watson, G. Wu, M. G. Richmond, *Organometallics* **2006**, *25*, 930.
- [36] W. H. Watson, G. Wu, M. G. Richmond, *Organometallics* **2005**, *24*, 5431.
- [37] W. H. Watson, B. Poola, M. G. Richmond, *J. Organomet. Chem.* **2006**, *691*, 4676.
- [38] X. Zhang, S. Kandala, L. Yang, W. H. Watson, X. Wang, D. A. Hrovat, W. T. Borden, M. G. Richmond, *Organometallics* **2011**, *30*, 1253.
- [39] a) M. R. Churchill, R. A. Lashewycz, S. I. Richter, J. R. Shapley, *Inorg. Chem.* **1980**, *19*, 1277; b) J. Puga, A. Arce, D. Braga, N. Centritto, F. Grepioni, R. Castillo, J. Ascanio, *Inorg.*

- Chem.* **1987**, *26*, 867; c) P. Homanen, R. Persson, M. Haukka, T. A. Pakkanen, E. Nordlander, *Organometallics* **2000**, *19*, 5568.
- [40] T. F. Doumani, Patent no: 2,532,612, **1945**, United States Patent Office, USA.
- [41] M. J. Frisch, G. W. Trucks, H. B. Schlegel, G. E. Scuseria, M. A. Robb, J. R. Cheeseman, G. Scalmani, V. Barone, B. Mennucci, G. A. Petersson, H. Nakatsuji, M. Caricato, X. Li, H. P. Hratchian, A. F. Izmaylov, J. Bloino, G. Zheng, J. L. Sonnenberg, M. Hada, M. Ehara, K. Toyota, R. Fukuda, J. Hasegawa, M. Ishida, T. Nakajima, Y. Honda, O. Kitao, H. Nakai, T. Vreven, J. A. Montgomery, Jr., J. E. Peralta, F. Ogliaro, M. Bearpark, J. J. Heyd, E. Brothers, K. N. Kudin, V. N. Staroverov, R. Kobayashi, J. Normand, K. Raghavachari, A. Rendell, J. C. Burant, S. S. Iyengar, J. Tomasi, M. Cossi, N. Rega, J. M. Millam, M. Klene, J. E. Knox, J. B. Cross, V. Bakken, C. Adamo, J. Jaramillo, R. Gomperts, R. E. Stratmann, O. Yazyev, A. J. Austin, R. Cammi, C. Pomelli, J. W. Ochterski, R. L. Martin, K. Morokuma, V. G. Zakrzewski, G. A. Voth, P. Salvador, J. J. Dannenberg, S. Dapprich, A. D. Daniels, O. Farkas, J. B. Foresman, J. V. Ortiz, J. Cioslowski, D. J. Fox, *Gaussian 09*, Revision A.02, Gaussian, Inc., Wallingford, CT, **2009**.
- [42] A. D. Becke, *J. Chem. Phys.* **1993**, *98*, 5648.
- [43] C. Lee, W. Yang, R. G. Parr, *Phys. Rev. B* **1988**, *37*, 785.
- [44] a) *JIMP2*, v. 0.091, a free program for the visualization and manipulation of molecules: M. B. Hall, R. F. Fenske, *Inorg. Chem.* **1972**, *11*, 768; b) J. Manson, C. E. Webster, M. B. Hall, Texas A&M University, College Station, TX, **2006**: <http://www.chem.tamu.edu/jimp2/index.html>.
- [45] A. C. T. North, D. C. Phillips, F. S. Mathews, *Acta Crystallogr., Sect. A: Cryst. Phys. Diffr., Theor. Gen. Crystallogr.* **1968**, *24*, 351.
- [46] G. M. Sheldrick, *SHELXS 97, Program for crystal structure solution*, University of Göttingen, Germany, **1997**.
- [47] G. M. Sheldrick, *SHELXL-97, Program for crystal structure refinement*, University of Göttingen, Germany, **1997**.
- [48] G. M. Sheldrick, *SADABS, Program for empirical absorption correction*, University of Göttingen, Germany, **1996**.
- [49] *SIR97, A new tool for crystal structure determination and refinement*: A. Altomare, M. C. Burla, M. Camalli, G. L. Cascarano, C. Giacovazzo, A. Guagliardi, A. G. G. Moliterni, G. R. Polidori Spagna, *J. Appl. Crystallogr.* **1999**, *32*, 115.
- [50] G. M. Sheldrick, *SHELXTLplus*, v. 5.1 (Windows® NT version), Structure Determination Package, Bruker Analytical X-ray Instruments Inc., Madison, WI, USA, **1998**.

Received: November 19, 2012  
Published Online: March 1, 2013